JCI The Journal of Clinical Investigation

Delayed reinforcement of costimulation improves the efficacy of mRNA vaccines in mice

Sarah Sanchez, … , Slim Fourati, Pablo Penaloza-MacMaster

J Clin Invest. 2024. https://doi.org/10.1172/JCI183973.

Research In-Press Preview Immunology

Graphical abstract

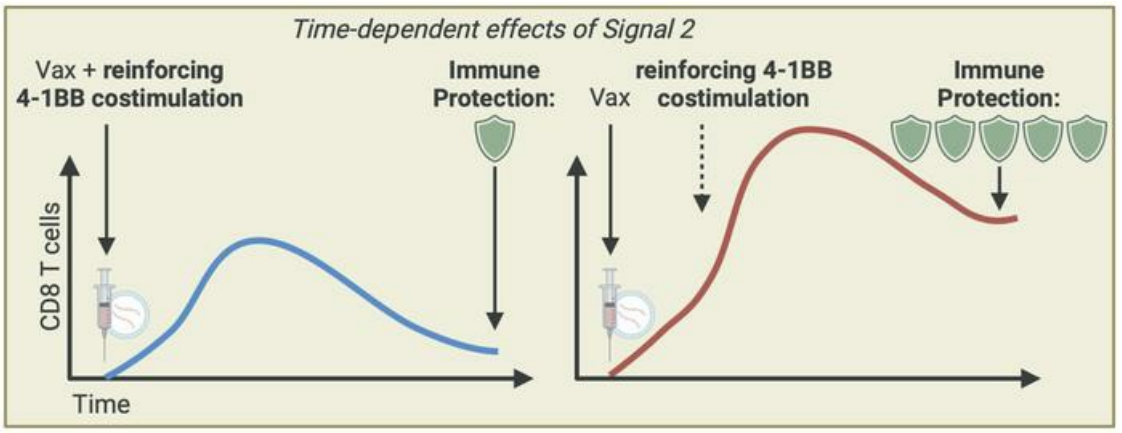

Delayed reinforcement of costimulation improves the efficacy of mRNA vaccines in mice

Sarah Sanchez[1], Tanushree Dangi[1], Bakare Awakoaiye[1], Min Han Lew[1], Nahid Irani[1], Slim Fourati[2], Pablo Penaloza-MacMaster*[1]

[1]Department of Microbiology-Immunology, Feinberg School of Medicine, Northwestern University, Chicago, IL 60611, USA. [2]Department of Medicine, Division of Allergy and Immunology, Feinberg School of Medicine and Center for Human Immunobiology, Northwestern University, Chicago, IL 60611, USA.

***Correspondence:**

Pablo Penaloza-MacMaster (ppm@northwestern.edu)

303 E. Chicago Ave. Tarry 6-728, Chicago, IL 60611

Phone: (312) 503-0357

Short Title:

Delayed 4-1BB improves vaccines

Abstract:

mRNA vaccines have demonstrated efficacy during the COVID-19 pandemic and are now being investigated for multiple diseases. However, concerns linger about the durability of immune responses, and the high incidence of breakthrough infections among vaccinated individuals highlights the need for improved mRNA vaccines. In this study, we investigated the effects of reinforcing costimulation via 4-1BB, a member of the TNF receptor superfamily, on immune responses elicited by mRNA vaccines. We first immunized mice with mRNA vaccines, followed by treatment with 4-1BB costimulatory antibodies to reinforce the 4-1BB pathway at different timepoints post-vaccination. Consistent with prior studies, reinforcing 4-1BB costimulation on the day of vaccination did not result in a substantial improvement of vaccine responses. However, reinforcing 4-1BB costimulation at day 4 post-vaccination, when 4-1BB expression levels were highest, resulted in a profound improvement of CD8 T cell responses associated with enhanced protection against pathogen challenges. A similar clinical benefit was observed in a therapeutic cancer vaccine model. We also report time-dependent effects with OX40, another costimulatory molecule of the TNF receptor superfamily. These findings demonstrate that delayed reinforcement of costimulation may exert an immunologic benefit, providing insights for the development of more effective mRNA vaccines for infectious diseases and cancer.

INTRODUCTION

mRNA lipid nanoparticle (mRNA-LNP) vaccines are used to prevent severe SARS-CoV-2 infection and are being explored for multiple diseases such as influenza, HIV-1, and cancer (1-3). While mRNA vaccines have shown efficacy in preventing COVID-19, they do not always confer complete protection as shown by the high incidence of breakthrough infections among vaccinated individuals, and their protection wanes over time, requiring multiple boosters. These limitations underscore the need to develop improved mRNA vaccine regimens. After vaccination, T cells play a critical role in rapidly clearing infected cells, and prior studies have shown that T cell responses are associated with reduced disease severity following breakthrough SARS-CoV-2 infection (4-6). According to the classical 2-signal model first described by Bretscher and colleagues, T cell responses are dependent on two concurrent signals: Naïve T cells must recognize their cognate antigen via their T cell receptor, and at the same time, they must receive costimulation (7). This model has been instrumental to understand how adaptive immune responses are generated and has had broad implications for the development of immunotherapies and vaccine adjuvants to reinforce costimulation at the time of priming. This model has also motivated the use of costimulatory regimens (e.g. costimulatory antibodies) to improve T cell responses after vaccination, but limited efficacy has been reported (8-12).

The most widely studied costimulatory pathway is CD28/B7, and the effects of other costimulatory pathways like 4-1BB/4-1BBL remain poorly understood. 4-1BB (also known as CD137) is a costimulatory receptor member of the tumor necrosis factor receptor superfamily (TNFRSF) and plays a role in T cell responses. 4-1BB is highly expressed on T cells and NK cells, among other

cells, whereas its ligand (4-1BBL) is expressed mostly on antigen presenting cells (13, 14). 4-1BB costimulation is important for effector T cell responses following bacterial and viral infections, and triggering of this pathway results in increased T cell proliferation, survival, and effector functions (10, 15-18). Prior studies have shown that 4-1BB costimulation renders T cells resistant to suppression by T regulatory cells (19), and due to its immunostimulatory effects, 4-1BB costimulatory antibodies have also been explored in cancer immunotherapy and for the treatment of chronic infection (16, 20-23). However, the effects of 4-1BB on vaccine responses remain incompletely understood, with some reports showing detrimental effects of 4-1BB on vaccine responses (8-12). Here, we studied the effects of 4-1BB costimulation on immune responses elicited by mRNA vaccines. Like prior studies, we show that triggering 4-1BB costimulation on the day of mRNA vaccination does not significantly improve vaccine responses. However, we show that triggering 4-1BB costimulation at day 4 post-vaccination, the time of maximal 4-1BB expression, significantly improves the efficacy of mRNA vaccines, rendering these vaccines more protective against breakthrough infections. These studies highlight a strategy to improve mRNA vaccines via time-dependent modulation of 4-1BB and suggest potential benefits of delaying 4-1BB costimulation for optimal CD8 T cell expansion.

RESULTS

Delayed 4-1BB costimulation induces a significant improvement of vaccine-elicited CD8 T cells.

Antigen recognition and costimulation are two indispensable signals needed for T cell responses, as the absence of costimulation results in anergy (24). While conventional wisdom from the classical 2-signal model is that antigen recognition and costimulation should occur simultaneously, the optimal timing of costimulation after antigen recognition remains unclear. We conducted experiments to investigate how the timing of 4-1BB costimulation affects immune responses after mRNA vaccination. We primed C57BL/6 mice intramuscularly with an mRNA vaccine expressing the SARS-CoV-2 spike protein (mRNA-spike) similar to the Moderna and Pfizer-BioNTech vaccines, and on the same day, we treated these mice intraperitoneally with 4-1BB costimulatory antibodies or control antibodies to examine the effect of reinforcing 4-1BB costimulation during the early priming phase (**Supplemental Figure 1A**). Reinforcing 4-1BB costimulation during the early priming phase did not improve CD8 T cell responses relative to control (**Supplemental Figure 1B**) and exerted a negative effect on antibody responses (**Supplemental Figure 1C**). Like many other costimulatory receptors, 4-1BB is an activation-induced molecule (25), motivating us to examine whether reinforcing 4-1BB costimulation later during the immune response would improve vaccine responses (**Figure 1A**). Interestingly, treatment with 4-1BB costimulatory antibodies at day 4 post-vaccination resulted in a potent and durable increase of CD8 T cell responses in blood (**Figure 1, B and C**) and tissues (**Supplemental Figure 2, A-C**). This potentiation of CD8 T cell responses was associated with higher Ki67 and PD-1 expression, suggesting enhanced proliferation and activation (**Supplemental Figure 2, D and E**). Treatment

with 4-1BB costimulatory antibodies at day 4 post-vaccination also improved degranulation and cytokine expression capacity on virus-specific CD8 T cells (**Supplemental Figure 2, F-I**) and CD4 T cells (**Supplemental Figure 2J**). There were no significant differences in the frequencies of short-lived effector cells (SLEC) and memory precursor effector cells (MPEC) (**Supplemental Figure 2, K and L**).

In addition, treatment with 4-1BB costimulatory antibodies at day 4 post-vaccination resulted in a significant increase in systemic cytokines, especially GM-CSF, relative to control vaccination (**Supplemental Figure 3A**). Although GM-CSF was significantly upregulated after α4-1BB treatment, GM-CSF blockade did not abrogate the positive effect of α4-1BB on vaccine-elicited CD8 T cells (**Supplemental Figure 3, B and C**). Reinforcing 4-1BB costimulation also upregulated IFNγ (**Supplemental Figure 3A**), which is known to downmodulate mRNA→protein translation (26). Therefore, we interrogated whether treatment with α4-1BB could reduce antigen expression after mRNA vaccination. To investigate this possibility, we measured antigen expression using an mRNA-LNP encoding a luciferase reporter. Our data show that α4-1BB treatment does not significantly alter antigen expression following mRNA vaccination (**Supplemental Figure 4**).

In the studies above, we administered a single low dose of 4-1BB costimulatory antibodies (50 μg) that was previously titrated to saturate all 4-1BB receptors for 3 days (16). Higher and repetitive doses of 4-1BB costimulatory antibodies (200 μg on days 4, 7, and 10) did not further improve CD8 T cell responses relative to single treatment at day 4 (**Supplemental Figure 5, A and B**). Administration of 4-1BB costimulatory antibodies at day 4 did not significantly affect antibody

responses after mRNA vaccination (**Supplemental Figure 5C**). Moreover, treatment with 4-1BB costimulatory antibodies after 2 weeks post-vaccination (contraction phase) did not affect immune responses (**Supplemental Figure 6**), demonstrating that the positive effects of 4-1BB costimulatory antibodies were time-dependent. Altogether, day 4 was a critical time point to costimulate CD8 T cells via 4-1BB, and further costimulation at later days did not confer an additional benefit.

Effects of 4-1BB costimulation on CD8 T cell differentiation.

Following an initial antigen encounter, CD8 T cells differentiate into distinct subsets, including effector (Teff), effector memory (Tem), and central memory cells (Tcm) (27-29). To examine whether reinforcing 4-1BB costimulation selectively favored the differentiation of specific subsets, we FACS-sorted splenic virus-specific CD8 T cells at day 7 post-vaccination and performed RNA-sequencing (RNA-seq) analyses. By principal component analyses (PCA), virus-specific CD8 T cells clustered differently, suggesting transcriptional differences (**Figure 2A**). We observed enrichment of genes associated with cell proliferation, activation, and effector differentiation (**Figure 2, B-E**), and more pronounced effector signatures by gene set enrichment analyses (GSEA) (**Figure 2F**) in mice that received 4-1BB costimulatory antibodies at day 4. We validated these gene expression results at the protein level using flow cytometry. Consistent with the gene expression data, virus-specific CD8 T cells after 4-1BB costimulation exhibited more pronounced effector (CD62L- CD127-) and effector memory (CD62L- CD127+) differentiation (**Figure 2, G-H**). There was a pattern of increased central memory CD8 T cells (CD62L+ CD127+) in mice that received α4-1BB, but the differences were not statistically significant relative to

control (**Figure 2I**). Effector and effector memory CD8 T cells were significantly greater in mice that received α4-1BB, relative to control (**Figure 2, J and K**).

Generalizability to other vaccines

We then interrogated the generalizability of our observations using other mRNA-based vaccines. Consistent with the prior data, 4-1BB costimulation at day 4 resulted in a significant improvement of CD8 T cells following vaccination with an mRNA vaccine against lymphocytic choriomeningitis virus (LCMV) (**Figure 3A**), and most virus-specific CD8 T cells exhibited an effector and effector memory phenotype (**Figure 3, B and C**). Reinforcing 4-1BB costimulation at day 4 post-vaccination also resulted in a significant improvement of CD8 T cells following immunization with other mRNA vaccines, including a common cold coronavirus (OC43) vaccine (**Figure 3D**), a human immunodeficiency virus (HIV-1) vaccine (**Figure 3E**), and an ovalbumin (OVA) vaccine (**Figure 3F**). No statistically significant differences were observed in CD4 T cell and antibody responses (**Supplemental Figure 7**). These data with multiple mRNA vaccines suggest that delayed 4-1BB costimulation was beneficial for CD8 T cell responses.

We validated these observations with a different vaccine platform, a poxvirus vector used in the clinically approved Mpox vaccine that is based on modified vaccinia Ankara (MVA). Consistent with our prior studies with mRNA vaccines, we also observed improvement of poxvirus-specific CD8 T cell responses when mice were treated with 4-1BB costimulatory antibodies at day 4 post-vaccination (**Supplemental Figure 8, A and B**). No difference was observed in poxvirus-specific antibody responses (**Supplemental Figure 8C**). Furthermore, we tested an MVA-vectored vaccine expressing the SARS-CoV spike antigen derived from the original coronavirus of 2004 (MVA-

SARS-1 spike) (**Supplemental Figure 8D**). With this vaccine, we also observed improvement of CD8 T cell responses but no difference in antibodies when 4-1BB was reinforced at day 4 post-vaccination (**Supplemental Figure 8, E and F**). Taken together, we show in multiple vaccine platforms that 4-1BB costimulation at day 4 post-vaccination results in an improvement of CD8 T cell responses.

Kinetics of 4-1BB on vaccine-elicited CD8 T cells

We interrogated whether the time-dependent effects of 4-1BB costimulation were linked to varying expression levels of 4-1BB on CD8 T cells. To answer this question, we measured 4-1BB expression on virus-specific CD8 T cells at various timepoints post-vaccination to determine whether there was a direct association between 4-1BB levels and response to 4-1BB costimulation. Since virus-specific CD8 T cells cannot be detected at day 4 post-vaccination due to low precursor frequency, we utilized an adoptive transfer model using P14 cells, which allowed us to examine virus-specific CD8 T cells at hyperacute timepoints (**Figure 3G**). Interestingly, 4-1BB expression exhibited "zig-zag" kinetics, peaking on day 4 and returning to baseline levels by day 7 post-vaccination (**Figure 3H**). Altogether, our data suggest that triggering 4-1BB at the time of maximal 4-1BB expression was beneficial for CD8 T cell responses.

Reinforcing 4-1BB costimulation at day 4 post-vaccination confers enhanced vaccine protection against antigen challenges

SARS-CoV-2 vaccines confer robust protection in k18-hACE2 mice, making them unsuitable for examining differences in immune protection after 4-1BB costimulation. Thus, we utilized more stringent pathogen challenges to compare vaccine protection. We first vaccinated mice with an

mRNA vaccine against LCMV and then treated these mice with α4-1BB or control antibodies at day 4 post-vaccination (**Figure 4A**). After 2 weeks, we challenged these mice intravenously (i.v.) with a high dose of chronic LCMV Cl-13 and then measured weight loss and viral loads at day 7 post-challenge (**Figure 4A**). Strikingly, most of the mice that received 4-1BB costimulation at day 4 post-vaccination exhibited complete protection against this stringent arenavirus challenge (**Figure 4B and Supplemental Figure 9**). We validated these results with a different vaccine model, by vaccinating mice with an mRNA vaccine expressing OVA and then challenging them i.v. with listeria monocytogenes expressing OVA (LM-OVA) (**Figure 4C**). Mice that received 4-1BB costimulatory antibodies exhibited complete protection upon challenge with a supra-lethal dose of LM-OVA (**Figure 4D**). These data suggested that delayed 4-1BB costimulation at day 4 post-vaccination rendered the vaccines fully protective. Taken together, reinforcing 4-1BB on day 4 post-vaccination, the time of maximal 4-1BB expression, potentiated CD8 T cell responses and enabled them to more effectively protect the host upon subsequent pathogen challenges.

We also examined the effects of α4-1BB during a booster vaccination by re-administering these costimulatory antibodies after a booster vaccination (Figure S10A). Following booster vaccination there was a robust increase in recall CD8 T cell responses in both groups and α4-1BB did not confer a significant benefit (Figure S10B). These data suggest that memory CD8 T cells may be less reliant on 4-1BB costimulation for their recall expansion, relative to naïve CD8 T cells. Another consideration is that 4-1BB costimulatory antibodies have been explored for various diseases, but their high toxicity profiles have precluded them from being licensed. Prior studies have shown that treatment with 4-1BB costimulatory antibodies can cause hepatotoxicity linked to increase in liver enzyme activity such as alanine aminotransferase (ALT) (25, 30), so we

interrogated whether our low dose α4-1BB regimen would induce a similar detrimental effect. With the single low dose tested in our vaccine studies (50 μg given at day 4 post-prime), we did not observe upregulation of liver enzyme activity (ALT) relative to control, suggesting that this low dose treatment was safe and well tolerated (**Supplemental Figure 11**).

We performed additional experiments to interrogate whether delayed 4-1BB costimulation improves tumor control in a therapeutic cancer vaccine model. To answer this question, we first challenged mice subcutaneously with B16-OVA tumor cells. After the tumor was established, mice were immunized with an mRNA-OVA vaccine, and then treated with α4-1BB at day 0 or day 4 post-vaccination to determine whether the timing of α4-1BB affected tumor control (**Figure 5A**). α4-1BB at day 0 post-vaccination improved tumor control relative to vaccination alone, but the enhancement in tumor control was more significant when α4-1BB was administered at day 4 post-vaccination (**Figure 5B**). Mice that received α4-1BB at day 4 post-vaccination also exhibited improved survival relative to all groups (**Figure 5C**), and this was associated with enhanced CD8 T cell responses (**Figure 5, D and E**), especially effector CD8 T cell responses ($p=0.0003$, **Figure 5, F-H**).

We then interrogated whether our observations could generalize to other costimulatory molecules. Interestingly, OX40, which is also a member of the TNFRSF, exhibited the same "zig-zag" kinetics as 4-1BB: its expression on virus-specific CD8 T cells was highest on day 4 and returned to baseline levels by day 7 post-vaccination (**Figure 6, A and B**). A prediction from these kinetics data is that the optimal timepoint for OX40 costimulation is day 4 post-vaccination, since this timepoint corresponded to the peak expression of this molecule. To determine whether our

prediction was correct, we immunized C57BL/6 mice with an mRNA vaccine, and at day 0 or day 4 post-vaccination, we administered OX40 costimulatory antibodies to reinforce OX40 costimulation at these different time points (**Figure 6C**). Reinforcing OX40 costimulation on the day of vaccination did not significantly improve CD8 and CD4 T cell responses, but reinforcing OX40 costimulation on day 4 resulted in a significant improvement in these responses (**Figure 6D and Supplemental Figure 12**). Moreover, reinforcing OX40 costimulation at day 4 resulted in superior antibody responses than reinforcing OX40 costimulation at day 0 (**Figure 6E**). Although there was a pattern of improved antibody responses with αOX40 at day 4, relative to control or α4-1BB at day 4, the difference was not statistically significant (**Supplemental Figure 13**).

DISCUSSION

mRNA vaccines have been administered to millions of people worldwide and have shown efficacy in preventing severe disease and death caused by SARS-CoV-2 infection. However, these vaccines do not confer complete protection and require multiple booster shots, underscoring the need for improved mRNA vaccines. In this study, we interrogated whether mRNA vaccines could be improved by reinforcing 4-1BB, a costimulatory molecule that is important for T cell activation. 4-1BB costimulatory antibodies have been clinically tested in autoimmunity and cancer immunotherapy (22, 23), and the signaling molecules involved in 4-1BB costimulation are included in chimeric antigen receptor (CAR) T cell therapies (31). Although 4-1BB is known to play a costimulatory role, there are reports of 4-1BB causing immunosuppression when delivered concomitantly with antigen. For example, a prior study reported that when 4-1BB costimulatory antibodies are administered at the time of LCMV infection, both T cell and antibody responses are impaired (32). Similarly, other studies have shown impaired immune responses when 4-1BB costimulation is reinforced at the time of vaccination, hindering the exploration of 4-1BB agonistic regimens as vaccine adjuvants (8, 9). The potentially detrimental effects of combining costimulation concurrently with antigen priming may not be exclusive to 4-1BB. Prior studies have shown that reinforcing CD40 or OX40 costimulation on the day of priming with LCMV leads to impaired immune responses (33, 34). Considering our data and that of others, we hypothesized that concurrent provision of Signal 1 and Signal 2 may not be optimal for vaccine-elicited immune responses and that temporally separating these signals may be necessary to fully unleash the immunostimulatory effects of costimulation.

Antigen recognition is metaphorically analogous to inserting the key to turn on a car, while costimulation is analogous to stepping on the accelerator. Employing this classical analogy, inserting the key and stepping on the accelerator at the same time can lead to "flooding of the engine." This concept led us to hypothesize that extending the time interval between antigen recognition and costimulation would allow CD8 T cells to "warm up" and upregulate their costimulatory receptors, rendering them more responsive to subsequent costimulation. Our kinetics data corroborate the inducible nature of 4-1BB following vaccination, and we observe that a temporal separation between vaccination and 4-1BB costimulation improves the protective efficacy of mRNA vaccines. In other words, such positive time-dependent effects could be explained by the fact that 4-1BB is an inducible costimulatory receptor (25). Thus, 4-1BB costimulatory antibodies may not engage many 4-1BB receptors on naïve CD8 T cells since these cells have not yet upregulated 4-1BB on their surface. However, treatment with 4-1BB costimulatory antibodies at day 4 (when CD8 T cells express high levels of 4-1BB) may trigger more potent costimulatory signaling, leading to a more robust expansion of CD8 T cells. The inducible nature of 4-1BB as well as other costimulatory receptors likely ensures the proper sequence of signaling events, precluding "out-of-order" signaling (e.g. costimulation preceding antigen recognition).

We also examined the specific CD8 T cell subsets that were increased by α4-1BB. We show that α4-1BB at day 4 results in significant increase of effector CD8 T cells. These data are consistent with a prior study from the Watts laboratory showing that 4-1BB is important for the persistence of effector CD8 T cells in tissues (35). A cardinal feature of effector and effector memory CD8 T cells is their "response-ready" state (27) which provides rapid protection from breakthrough

infection, but these cells may have a shorter lifespan than central memory CD8 T cells. Notwithstanding the lower durability of effector memory CD8 T cells relative to central memory CD8 T cells, we detected increased CD8 T cell responses after 2 months of vaccination in mice that received 4-1BB costimulatory antibodies, suggesting long-term enhancement of responses by 4-1BB costimulation. Future studies will examine the durability of CD8 T cell responses over longer periods of time.

The complete protection observed in the chronic LCMV challenge and listeria challenge models is likely not only due to a numerical increase in antigen-specific CD8 T cells. As mentioned earlier, 4-1BB costimulation triggers qualitatively distinct CD8 T cells, characterized by enhanced effector memory differentiation. This type of memory response is known to exhibit rapid cytotoxic function which can quickly eliminate initial foci of infection, unlike other subsets that require a longer time to kill virally infected cells (27). Importantly, effector memory CD8 T cells are positioned in blood and tissues (36), rendering them able to protect against systemic or mucosal challenges. Replicating cytomegalovirus (CMV) vectors trigger similar effector memory CD8 T cell responses shown to protect against SIV infection in 50% of vaccinated macaques (37-40), but replicating vectors raise safety concerns so elucidating alternative strategies to generate effector memory CD8 T cells has been of interest in HIV vaccinology. As suggested by Masopust and Picker, vaccines against rapidly replicating intracellular pathogens (such as HIV, LCMV, or listeria) are thought to necessitate effector memory CD8 T cells to quickly control infection before the pathogen undergoes exponential replication (41). The observation that 4-1BB costimulation elicits effector and effector memory CD8 T cells could prove useful for an HIV vaccine, because these subsets are especially poised for rapid killing of virally infected cells at frontline tissues. Overall,

enhancing CD8 T cells by α4-1BB may translate into better protection from symptomatic SARS-CoV-2 disease, considering their established role in reducing disease severity by eliminating infected cells and not necessarily by preventing initial infection, as that would be a function of antibodies (6, 42).

The classical 2-signal model postulates that T cell activation is dependent on two concurrent signals, antigen recognition and costimulation, also known as Signal 1 and Signal 2, respectively (7). For decades, this model has been a blueprint for understanding how T cell responses are generated and has had broad implications for the development of immunotherapies and vaccine adjuvants aimed at triggering costimulation. However, it is currently believed that both signals must occur concurrently, exactly at the same time, otherwise the T cell would undergo anergy. Our data show potential benefits of delaying costimulation, but future studies are needed to determine the generalizability of these findings to other costimulatory pathways besides 4-1BB or OX40. Overall, these studies may be important for the development of more effective vaccines and for understanding the time-dependent effects of 4-1BB costimulation.

Limitations of the study. A potential limitation of our findings is the need for vaccinees to undergo an additional injection with costimulatory antibodies 4 days after initial vaccination. To address this logistical challenge, future studies will examine the effects of encapsulating 4-1BB costimulatory antibodies in slow-release formulations, which could be co-administered with the vaccine on the same day. Another consideration is that 4-1BB costimulatory antibodies can induce inflammation, which is a reason why 4-1BB costimulatory antibodies have not yet been licensed (25). However, in our studies we used a single low dose of 4-1BB costimulatory antibodies, and

we showed that the effects on vaccine responses were similar to when we administered high, repetitive doses, suggesting that the single low dose goes a long way. We also did not observe increase in ALT activity with our single low dose of α4-1BB relative to control, further suggesting that the single low dose regimen was safe, but further studies are needed to determine safety more rigorously.

MATERIALS AND METHODS

Sex as a biological variable. Our study examined male and female animals, and similar findings are reported for both sexes.

Mice, vaccinations, and antibody treatments

Sex as a biological variable: Our study examined male and female animals, and similar findings are reported for both sexes. 6-8-week-old C57BL/6 mice were used. Mice were purchased from Jackson laboratories (approximately half males and half females). Mice were immunized intramuscularly with mRNA-LNPs (made in-house) or MVA vectors (from Dr. Bernard Moss, NIH) diluted in sterile PBS. Mice received α4-1BB agonistic antibody (clone 3H3, BioXcell) or IgG control antibody (clone 2A3, BioXcell) intraperitoneally at 50 μg or 200 μg per mouse on the indicated days, diluted in sterile PBS. To block GM-CSF, we treated mice with an αGM-CSF blocking antibody (clone MP1-22E9, Leinco) intraperitoneally at 500 μg per mouse on days 4 and 7 post-vaccination. We utilized OX40 costimulatory antibody clone OX-86 from Leinco Technologies Inc (Cat no. C855). Mice were housed at Northwestern University's Center for Comparative Medicine (CCM) or University of Illinois at Chicago (UIC). All mouse experiments were performed with the approval of the Northwestern University Institutional Animal Care and Use Committee (IACUC).

Reagents, flow cytometry, and equipment

Single cell suspensions were obtained from PBMCs, and various tissues as described previously. Dead cells were gated out using Live/Dead fixable dead cell stain (Invitrogen). SARS-CoV-2 spike

and SF162 peptide pools were used for intracellular cytokine staining (ICS) and these were obtained from BEI Resources. Biotinylated MHC class I monomers (K^bVL8, sequence VNFNFNGL; D^bGP33, sequence KAVYNFATC; D^bGP276, sequence SGVENPGGYCL; OVA, sequence SIINFEKL; K^bB8R, sequence TSYKFESV) were used for detecting virus-specific CD8 T cells, and were obtained from the NIH tetramer facility at Emory University. Cells were stained with fluorescently-labeled antibodies against CD8α (53-6.7 on PerCP-Cy5.5), CD44 (IM7 on FITC), CD62L (MEL-14 on PE-Cy7), CD127 (A7R34 on Pacific Blue), and tetramers (APC). TNFα (MP6-XT22 on PE-Cy7), IFNγ (XMG1.2 on APC), or Ki67 (SolA15 on PE-Cy7). Fluorescently-labeled antibodies were purchased from BD Pharmingen, except for anti-CD127 and anti-CD44 (which were from Biolegend). Flow cytometry samples were acquired with a Becton Dickinson Canto II or an LSRII and analyzed using FlowJo v10 (Treestar).

SARS-CoV-2 spike, SARS-CoV-1 spike, OVA, HIV (SF162) envelope, and MVA lysate-specific ELISA

Binding antibody titers were measured using ELISA as described previously (4, 43-48). In brief, 96-well flat bottom plates MaxiSorp (Thermo Scientific) were coated with 0.1μ/well of the respective spike protein, for 48 hr at 4ºC. For detection of MVA-specific antibody responses, MVA lysates were used as coating antigen (incubated for 48 hr at room temperature). Plates were washed with PBS + 0.05% Tween-20. Blocking was performed for 4 hr at room temperature with 200 μL of PBS + 0.05% Tween-20 + bovine serum albumin. 6μL of sera were added to 144 μL of blocking solution in the first column of the plate, 1:3 serial dilutions were performed until row 12 for each sample, and plates were incubated for 60 minutes at room temperature. Plates were washed three times followed by the addition of goat anti-mouse IgG horseradish peroxidase-conjugated

(Southern Biotech) diluted in blocking solution (1:5000), at 100 µL/well and incubated for 60 minutes at room temperature. Plates were washed three times and 100 µL /well of Sure Blue substrate (Sera Care) was added for approximately 8 minutes. The reaction was stopped using 100 µL/well of KPL TMB stop solution (Sera Care). Absorbance was measured at 450 nm using a Spectramax Plus 384 (Molecular Devices). SARS-CoV-2 spike protein was produced in-house using a plasmid produced under HHSN272201400008C and obtained from BEI Resources, NIAID, NIH: vector pCAGGS containing the SARS-related coronavirus 2; Wuhan-Hu-1 spike glycoprotein gene (soluble, stabilized); NR-52394. SARS-CoV-1 spike protein was obtained through BEI Resources, NIAID, NIH: SARS-CoV Spike (S) Protein deltaTM, Recombinant from Baculovirus, NR-722. OVA protein was purchased from Worthington Biochemical (cat. no. LS003049). HIV-SF162 protein was obtained through the NIH AIDS Reagent Program, Division of AIDS, NIAID, NIH: Human Immunodeficiency Virus Type 1 SF162 gp140 Trimer Protein, Recombinant from HEK293T Cells, ARP-12026, contributed by Dr. Leo Stamatatos.

mRNA-LNP vaccines

We synthesized mRNA vaccines encoding for the codon-optimized SARS-CoV-2 spike protein from USA-WA1/2020, OC43 spike protein, OVA from the SERPINB14 gene, HIV-1 SF162 envelope protein, or the LCMV GP. Constructs were purchased from Integrated DNA Technologies (IDT) or Genscript, and contained a T7 promoter site for in vitro transcription of mRNA. The sequences of the 5′- and -3′′-UTRs were identical to those used in a previous publication (44). All mRNAs were encapsulated into lipid nanoparticles using the NanoAssemblr Benchtop system (Precision NanoSystems) and confirmed to have similar encapsulation efficiency (∼95%). mRNA was diluted in Formulation Buffer (Catalog # NWW0043, Precision

NanoSystems) to 0.17 mg/mL and then run through a laminar flow cartridge with GenVoy ILM encapsulation lipids (Catalog # NWW0041, Precision NanoSystems) with N/P (Lipid mix/mRNA ratio of 4) at a flow ratio of 3:1 (RNA: GenVoy-ILM), with a total flow rate of 12 mL/min, to produce mRNA–lipid nanoparticles (mRNA-LNPs). mRNA-LNPs were evaluated for encapsulation efficiency and mRNA concentration using RiboGreen assay using the Quant-iT RiboGreen RNA Assay Kit (Catalog #R11490, Invitrogen, Thermo Fisher Scientific).

RNA-Seq Data Acquisition and Analysis

C57BL/6 mice were immunized with 3 μg of mRNA-SARS-CoV-2 spike, and at day 4, treated with 4-1BB agonistic antibody. At day 7, splenic CD8 T cells were MACS-sorted with a MACS negative selection kit (STEMCELL). Purified CD8 T cells were stained with K^bVL8 tetramer, live dead stain, and antibodies for CD8 and CD44 to gate on virus-specific CD8 T cells. Live, CD8+, CD44+, K^bVL8+ cells were FACS-sorted to ~99% purity on a FACS Aria cytometer (BD Biosciences) and delivered to Admera Health Biopharma for RNA extraction using Illumina 2x150 and RNA-seq using SMARTseq V4 with NexteraXT kit. After the library was sequenced, the output file in BCL format was converted to FASTQ files and aligned to the mouse genome to generate a matrix file using the Cell Ranger pipeline (10X Genomics). These upstream QC steps were performed by Dr. Slim Fourati at Northwestern University. Further analyses were performed in R using the Seurat package v4.0, as previously described (49). Terminal effector gene signatures were derived using the edgeR package (50), comparing effector memory to terminal effector CD8 T cells (51). Clusters representing less than 4% of each population were excluded from downstream analyses.

Adoptive transfer of P14 cells to measure expression kinetics of costimulatory molecules

CD8+ T cells from Thy1.1$^+$ P14 mice (PBMCs) were enriched using a CD8 MACS-negative selection kit (STEMCELL Technologies). ~40,000 P14 CD8$^+$ T cells were transferred intravenously into naïve Thy1.2$^+$ C57BL/6 recipient mice. Recipient mice were vaccinated intramuscularly with 3 μg of the mRNA-LCMV vaccine 24 hours later. PBMCs were collected at various time points to measure 4-1BB expression on donor (Thy1.1+) P14 T cells by flow cytometry.

Multiplex cytokine/chemokine assay

Blood samples were centrifugated at 15000 rpm for 10 min at 4°C to separate the serum. The serum samples were collected and frozen at -80°C until its use. A multiplex cytokines/chemokines kit was purchased from Mesoscale Diagnostics LLC and used for quantifying serum cytokines/chemokines.

Alanine aminotransferase (ALT) Assay

To detect serum alanine aminotransferase (ALT) activity, sera were obtained from vaccinated mice treated with α4-1BB or control antibodies. ALT activity was measured using a colorimetric ALT Assay kit (RayBiotech, cat. no. MA-ALT) following the manufacturer's instructions.

Challenge models

LCMV Cl-13 stocks were expanded in Vero-E6 cells (ATCC, catalog CRL-1586), using a protocol from a prior paper (52). LCMV titers were determined by plaque assay on Vero-E6 cell

monolayers. LCMV Cl-13 challenges were intravenously at 2 x 10^6 PFU/mouse, and listeria (LM-OVA) challenges were intravenously at 10^7 CFU/mouse.

LCMV quantification

Seed stock of LCMV Cl-13 was obtained from Dr. Rafi Ahmed's laboratory. The virus was propagated and tittered on BHK21 cells (ATCC, catalog CCL-10). BHK21 cells were passaged in DMEM with 10% Fetal bovine serum (FBS). Cells were inoculated with a low MOI (0.1) in 1% DMEM and incubated for 72 hr. Titers were determined by plaque assay on Vero-E6 cell monolayers. Sera and spleen were collected at various time points post-challenge. Infectious viral titers were determined by plaque assay using Vero-E6 cells. 5 x 10^5 Vero-E6 cells per well were seeded in 6-well plates in 10% DMEM media, monolayer was 90-100% confluent after 24 hr. The spleen was homogenized using a standard TissueRuptur homogenizer, and 10-fold serial dilutions of tissues were made and then transferred dropwise onto the cell monolayer. Sera dilutions were created in 10% DMEM media and added dropwise on the cell monolayer. 6-well plates were placed in a 37°C 5% CO_2 incubator for 1 hr and manually rocked every 10 minutes. A 1:1 agarose/2x199 monolayer was dispensed after 1 hr incubation and plates were incubated at 37°C 5% CO_2 for 96 hr. After 96 hr a 1:50 1% neutral red solution was added to a 1:1 agarose/2x199 mixture and overlayed onto plates. Plaques were counted the following day after agar overlay removal.

Listeria quantification

Spleens were collected from infected mice on day 3 post-challenge. Bacterial titers were quantified by homogenizing tissues through a 42 μm strainer and resuspended in 1% Triton. 10-fold serial dilutions were created in 1% Triton and added dropwise onto 6-well BHK agar plates. Plates were

manually rocked and then incubated at 37°C 5% CO_2 for 24 hours. Colonies were counted the next day.

B16-OVA melanoma model to study therapeutic vaccination

B16-OVA melanoma cells were a gift from Dr. Jennifer Wu (Northwestern University). Mice were injected subcutaneously with $2x10^6$ B16-OVA tumor cells used in prior studies (53). At day 10 post tumor challenge, mice were vaccinated intramuscularly with 3 μg of mRNA-OVA, followed by treatment with 50 μg of control antibodies or α4-1BB at different timepoints. Tumor volume was calculated as length × width × width × ½.

In vivo bioluminescence

We utilized an mRNA-LNP expressing a luciferase reporter (mRNA-luc) to examine whether 4-1BB affected antigen (luciferase) levels following mRNA vaccination. To quantify luciferase expression, luciferin (GoldBio, Catalog # LUCK-100) was administered intraperitoneally 15 min before imaging, as done previously (45, 54). Mice were anesthetized and imaged using a SII Lago IVIS Imager (Spectral Instruments Imaging). Region of interest (ROI) bioluminescence was used to quantify the signal. Each leg (quadriceps) was plotted as an individual immunization site.

Statistical analysis

Statistical tests used are indicated on each figure legend. Dashed lines in data figures represent the limit of detection. Data represent mean and error bars represent SEM. Statistical significance was established at $P \leq 0.05$. Data were analyzed using Prism version 10 (Graphpad).

Study approval

Mouse studies were performed at Northwestern University following biosafety level 2 guidelines with approval of the Institutional Animal Care and Use Committee under protocols IS00003324, IS00029076, IS00015002, IS00008785, and IS00003258.

Data availability

RNA-Seq accession data were deposited in the NCBI's Gene Expression Omnibus (GEO) database; under accession number GSE260817, at https://www.ncbi.nlm.nih.gov/geo/query/acc.cgi?acc=GSE260817 . Other data are available upon request. Supporting data values associated with the main article and supplemental material are included in the Supporting Data Values file.

Competing Interests: The authors declare no competing interests.

AUTHOR CONTRIBUTIONS

PPM and SS designed the experiments. SS performed most of the experiments. TD, MHL, NI and BA helped with some of the immunogenicity experiments. SF analyzed the gene expression data. PPM and SS wrote the manuscript with feedback from all authors.

ACKNOWLEDGEMENTS

We thank the late Dr. Robert Mittler for discussions. We also thank Drs. Arlene Sharpe and Tania Watts for discussions, and Dr. Thomas Gallagher for help designing the mRNA-OC43 vaccine. Dr. This work was possible with grants from the National Institute on Drug Abuse (NIDA, DP2DA051912), Third Coast Centers for AIDS Research (CFAR), and the National Institute of Allergy and Infectious Diseases (NIAID, 1R56AI187084) to P.P.M.

1. Chen J, Ye Z, Huang C, Qiu M, Song D, Li Y, et al. Lipid nanoparticle-mediated lymph node-targeting delivery of mRNA cancer vaccine elicits robust CD8(+) T cell response. *Proc Natl Acad Sci U S A.* 2022;119(34):e2207841119.
2. Arevalo CP, Bolton MJ, Le Sage V, Ye N, Furey C, Muramatsu H, et al. A multivalent nucleoside-modified mRNA vaccine against all known influenza virus subtypes. *Science.* 2022;378(6622):899-904.
3. Pardi N, Hogan MJ, Porter FW, and Weissman D. mRNA vaccines - a new era in vaccinology. *Nat Rev Drug Discov.* 2018;17(4):261-79.
4. Dangi T, Class J, Palacio N, Richner JM, and Penaloza MacMaster P. Combining spike- and nucleocapsid-based vaccines improves distal control of SARS-CoV-2. *Cell Rep.* 2021;36(10):109664.
5. Koutsakos M, Reynaldi A, Lee WS, Nguyen J, Amarasena T, Taiaroa G, et al. SARS-CoV-2 breakthrough infection induces rapid memory and de novo T cell responses. *Immunity.* 2023;56(4):879-92 e4.
6. Moss P. The T cell immune response against SARS-CoV-2. *Nat Immunol.* 2022;23(2):186-93.
7. Bretscher PA. A two-step, two-signal model for the primary activation of precursor helper T cells. *Proc Natl Acad Sci U S A.* 1999;96(1):185-90.
8. Hong JP, Reynoso GV, Andhey PS, Swain A, Turner JS, Boon ACM, et al. An Agonistic Anti-CD137 Antibody Disrupts Lymphoid Follicle Structure and T-Cell-Dependent Antibody Responses. *Cell Rep Med.* 2020;1(3).

9. Ganguly S, Liu J, Pillai VB, Mittler RS, and Amara RR. Adjuvantive effects of anti-4-1BB agonist Ab and 4-1BBL DNA for a HIV-1 Gag DNA vaccine: different effects on cellular and humoral immunity. *Vaccine.* 2010;28(5):1300-9.

10. Munks MW, Mourich DV, Mittler RS, Weinberg AD, and Hill AB. 4-1BB and OX40 stimulation enhance CD8 and CD4 T-cell responses to a DNA prime, poxvirus boost vaccine. *Immunology.* 2004;112(4):559-66.

11. Hirao LA, Hokey DA, Morrow MP, Jure-Kunkel MN, and Weiner DB. Immune modulation through 4-1BB enhances SIV vaccine protection in non-human primates against SIVmac251 challenge. *PLoS One.* 2011;6(9):e24250.

12. Ozpolat B, Rao XM, Powell MF, and Lachman LB. Immunoliposomes containing antibodies to costimulatory molecules as adjuvants for HIV subunit vaccines. *AIDS Res Hum Retroviruses.* 1998;14(5):409-17.

13. Croft M. The role of TNF superfamily members in T-cell function and diseases. *Nat Rev Immunol.* 2009;9(4):271-85.

14. Wilcox RA, Chapoval AI, Gorski KS, Otsuji M, Shin T, Flies DB, et al. Cutting edge: Expression of functional CD137 receptor by dendritic cells. *J Immunol.* 2002;168(9):4262-7.

15. Lee DY, Choi BK, Lee DG, Kim YH, Kim CH, Lee SJ, et al. 4-1BB signaling activates the t cell factor 1 effector/beta-catenin pathway with delayed kinetics via ERK signaling and delayed PI3K/AKT activation to promote the proliferation of CD8+ T Cells. *PLoS One.* 2013;8(7):e69677.

16. Vezys V, Penaloza-MacMaster P, Barber DL, Ha SJ, Konieczny B, Freeman GJ, et al. 4-1BB signaling synergizes with programmed death ligand 1 blockade to augment CD8 T cell responses during chronic viral infection. *J Immunol.* 2011;187(4):1634-42.

17. Myers L, Lee SW, Rossi RJ, Lefrancois L, Kwon BS, Mittler RS, et al. Combined CD137 (4-1BB) and adjuvant therapy generates a developing pool of peptide-specific CD8 memory T cells. *Int Immunol.* 2006;18(2):325-33.

18. Shuford WW, Klussman K, Tritchler DD, Loo DT, Chalupny J, Siadak AW, et al. 4-1BB costimulatory signals preferentially induce CD8+ T cell proliferation and lead to the amplification in vivo of cytotoxic T cell responses. *J Exp Med.* 1997;186(1):47-55.

19. Robertson SJ, Messer RJ, Carmody AB, Mittler RS, Burlak C, and Hasenkrug KJ. CD137 costimulation of CD8+ T cells confers resistance to suppression by virus-induced regulatory T cells. *J Immunol.* 2008;180(8):5267-74.

20. Claus C, Ferrara-Koller C, and Klein C. The emerging landscape of novel 4-1BB (CD137) agonistic drugs for cancer immunotherapy. *MAbs.* 2023;15(1):2167189.

21. Melero I, Shuford WW, Newby SA, Aruffo A, Ledbetter JA, Hellstrom KE, et al. Monoclonal antibodies against the 4-1BB T-cell activation molecule eradicate established tumors. *Nat Med.* 1997;3(6):682-5.

22. Yonezawa A, Dutt S, Chester C, Kim J, and Kohrt HE. Boosting Cancer Immunotherapy with Anti-CD137 Antibody Therapy. *Clin Cancer Res.* 2015;21(14):3113-20.

23. Melero I, Sanmamed MF, Glez-Vaz J, Luri-Rey C, Wang J, and Chen L. CD137 (4-1BB)-Based Cancer Immunotherapy on Its 25th Anniversary. *Cancer Discov.* 2023;13(3):552-69.

24. Schwartz RH. T cell anergy. *Annu Rev Immunol.* 2003;21:305-34.

25. Chester C, Sanmamed MF, Wang J, and Melero I. Immunotherapy targeting 4-1BB: mechanistic rationale, clinical results, and future strategies. *Blood.* 2018;131(1):49-57.

26. Su X, Yu Y, Zhong Y, Giannopoulou EG, Hu X, Liu H, et al. Interferon-gamma regulates cellular metabolism and mRNA translation to potentiate macrophage activation. *Nat Immunol.* 2015;16(8):838-49.

27. Wherry EJ, Teichgraber V, Becker TC, Masopust D, Kaech SM, Antia R, et al. Lineage relationship and protective immunity of memory CD8 T cell subsets. *Nat Immunol.* 2003;4(3):225-34.

28. Sallusto F, Geginat J, and Lanzavecchia A. Central memory and effector memory T cell subsets: function, generation, and maintenance. *Annu Rev Immunol.* 2004;22:745-63.

29. Geginat J, Lanzavecchia A, and Sallusto F. Proliferation and differentiation potential of human CD8+ memory T-cell subsets in response to antigen or homeostatic cytokines. *Blood.* 2003;101(11):4260-6.

30. Bartkowiak T, Jaiswal AR, Ager CR, Chin R, Chen CH, Budhani P, et al. Activation of 4-1BB on Liver Myeloid Cells Triggers Hepatitis via an Interleukin-27-Dependent Pathway. *Clin Cancer Res.* 2018;24(5):1138-51.

31. Singh R, Kim YH, Lee SJ, Eom HS, and Choi BK. 4-1BB immunotherapy: advances and hurdles. *Exp Mol Med.* 2024.

32. Zhang B, Maris CH, Foell J, Whitmire J, Niu L, Song J, et al. Immune suppression or enhancement by CD137 T cell costimulation during acute viral infection is time dependent. *J Clin Invest.* 2007;117(10):3029-41.

33. Bartholdy C, Kauffmann SO, Christensen JP, and Thomsen AR. Agonistic anti-CD40 antibody profoundly suppresses the immune response to infection with lymphocytic choriomeningitis virus. *J Immunol.* 2007;178(3):1662-70.

34. Boettler T, Choi YS, Salek-Ardakani S, Cheng Y, Moeckel F, Croft M, et al. Exogenous OX40 stimulation during lymphocytic choriomeningitis virus infection impairs follicular Th cell differentiation and diverts CD4 T cells into the effector lineage by upregulating Blimp-1. *J Immunol.* 2013;191(10):5026-35.

35. Zhou AC, Batista NV, and Watts TH. 4-1BB Regulates Effector CD8 T Cell Accumulation in the Lung Tissue through a TRAF1-, mTOR-, and Antigen-Dependent Mechanism to Enhance Tissue-Resident Memory T Cell Formation during Respiratory Influenza Infection. *J Immunol.* 2019;202(8):2482-92.

36. Masopust D, Vezys V, Marzo AL, and Lefrancois L. Preferential localization of effector memory cells in nonlymphoid tissue. *Science.* 2001;291(5512):2413-7.

37. Hansen SG, Marshall EE, Malouli D, Ventura AB, Hughes CM, Ainslie E, et al. A live-attenuated RhCMV/SIV vaccine shows long-term efficacy against heterologous SIV challenge. *Sci Transl Med.* 2019;11(501).

38. Hansen SG, Piatak M, Jr., Ventura AB, Hughes CM, Gilbride RM, Ford JC, et al. Immune clearance of highly pathogenic SIV infection. *Nature.* 2013;502(7469):100-4.

39. Hansen SG, Ford JC, Lewis MS, Ventura AB, Hughes CM, Coyne-Johnson L, et al. Profound early control of highly pathogenic SIV by an effector memory T-cell vaccine. *Nature.* 2011;473(7348):523-7.

40. Hansen SG, Vieville C, Whizin N, Coyne-Johnson L, Siess DC, Drummond DD, et al. Effector memory T cell responses are associated with protection of rhesus monkeys from mucosal simian immunodeficiency virus challenge. *Nat Med.* 2009;15(3):293-9.

41. Masopust D, and Picker LJ. Hidden memories: frontline memory T cells and early pathogen interception. *J Immunol.* 2012;188(12):5811-7.

42. Bertoletti A, Le Bert N, and Tan AT. SARS-CoV-2-specific T cells in the changing landscape of the COVID-19 pandemic. *Immunity.* 2022;55(10):1764-78.

43. Dangi T, Sanchez S, Class J, Richner MC, Visvabharathy L, Chung YR, et al. Improved control of SARS-CoV-2 by treatment with nucleocapsid-specific monoclonal antibody. *J Clin Invest.* 2022.

44. Dangi T, Palacio N, Sanchez S, Park M, Class J, Visvabharathy L, et al. Cross-protective immunity following coronavirus vaccination and coronavirus infection. *J Clin Invest.* 2021;131(24).

45. Dangi T, Sanchez S, Lew MH, Awakoaiye B, Visvabharathy L, Richner JM, et al. Pre-existing immunity modulates responses to mRNA boosters. *Cell Rep.* 2023;42(3):112167.

46. Tanushree Dangi SS, Jacob Class, Michelle Richner, Lavanya, Visvabharathy YRC, Kirsten Bentley, Richard J. Stanton, Igor J., and Koralnik JMR, Pablo Penaloza-MacMaster. Improved control of SARS-CoV-2 by treatment with nucleocapsid-specific monoclonal antibody. *The Journal of Clinical Investigation (in press).* 2022.

47. Dangi T, Chung, YR., Palacio, N., Penaloza-MacMaster, P. Interrogating Adaptive Immunity Using LCMV. *Current Protocols in Immunology.* 2020(130):1-37.

48. Palacio N, Dangi T, Chung YR, Wang Y, Loredo-Varela JL, Zhang Z, et al. Early type I IFN blockade improves the efficacy of viral vaccines. *J Exp Med.* 2020;217(12).

49. Ciucci T, Vacchio MS, Gao Y, Tomassoni Ardori F, Candia J, Mehta M, et al. The Emergence and Functional Fitness of Memory CD4(+) T Cells Require the Transcription Factor Thpok. *Immunity.* 2019;50(1):91-105 e4.

50. Robinson MD, McCarthy DJ, and Smyth GK. edgeR: a Bioconductor package for differential expression analysis of digital gene expression data. *Bioinformatics.* 2010;26(1):139-40.

51. Milner JJ, Nguyen H, Omilusik K, Reina-Campos M, Tsai M, Toma C, et al. Delineation of a molecularly distinct terminally differentiated memory CD8 T cell population. *Proc Natl Acad Sci U S A.* 2020;117(41):25667-78.

52. Dangi T, Chung YR, Palacio N, and Penaloza-MacMaster P. Interrogating Adaptive Immunity Using LCMV. *Curr Protoc Immunol.* 2020;130(1):e99.

53. Chung YR, Awakoaiye B, Dangi T, Irani N, Fourati S, and Penaloza-MacMaster P. An attenuated lymphocytic choriomeningitis virus vector enhances tumor control in mice partly via IFN-I. *J Clin Invest.* 2024;134(15).

54. Sanchez S, Palacio N, Dangi T, Ciucci T, and Penaloza-MacMaster P. Fractionating a COVID-19 Ad5-vectored vaccine improves virus-specific immunity. *Sci Immunol.* 2021;6(66):eabi8635.

Figures:

Figure 1

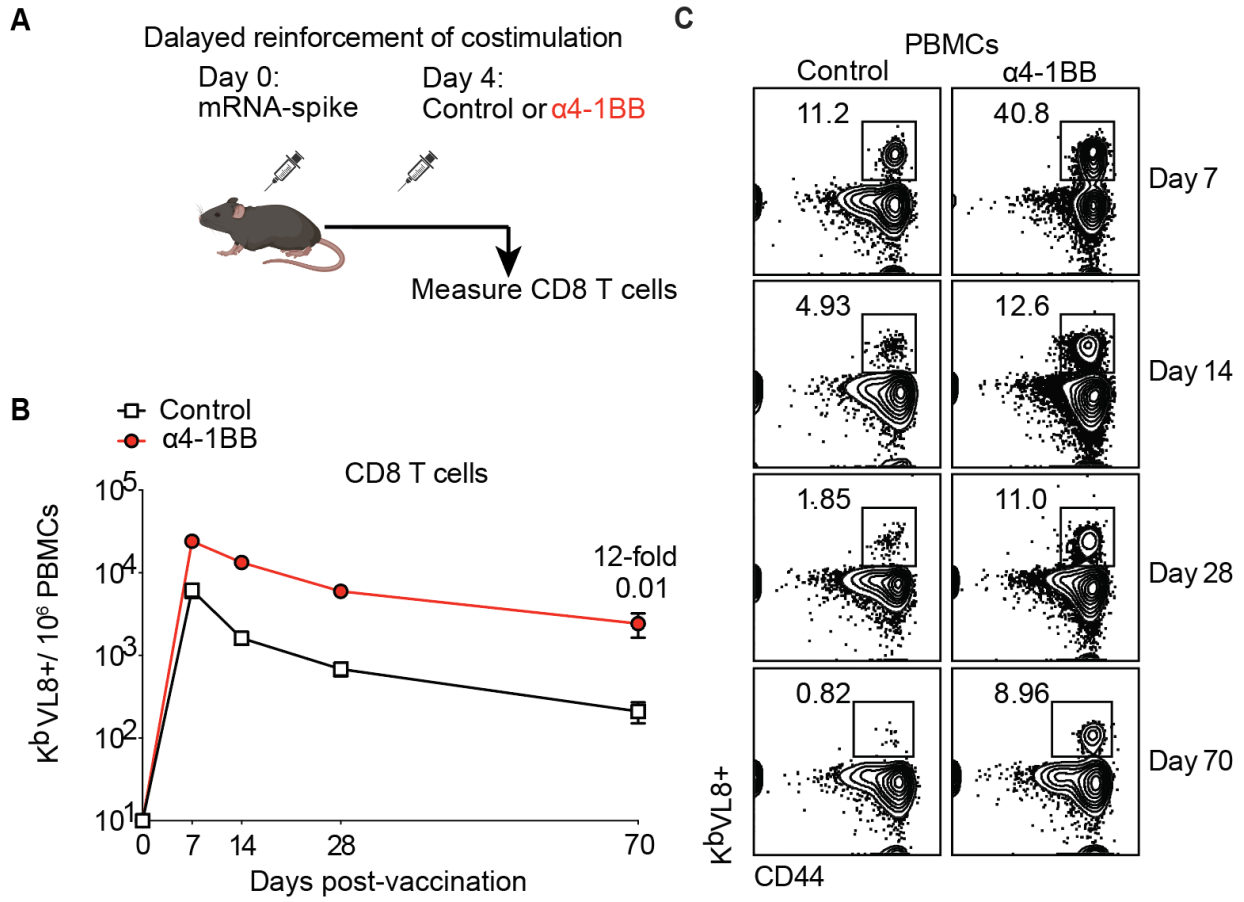

Figure 1. Reinforcing 4-1BB costimulation at day 4 post-vaccination increases the number and durability of CD8 T cell responses. (**A**) Experimental outline for evaluating whether treatment with α4-1BB at day 4 improves immune responses. Mice were immunized with 3 μg of an mRNA-spike vaccine followed by treatment with 50 μg of α4-1BB or control antibodies at day 4. (**B**) Summary of virus-specific CD8 T cells. (**C**) Representative FACS plots of virus-specific CD8 T cells. Data are from peripheral blood mononuclear cells (PBMCs). K^bVL8 (shown in the y-axis) is an MHC I tetramer used to detect SARS-CoV-2 spike-specific CD8 T cells. Data are from one experiment, n=4-5 per group/experiment; experiment was performed twice with similar results. Indicated P values were calculated by the Mann–Whitney test at the last time point.

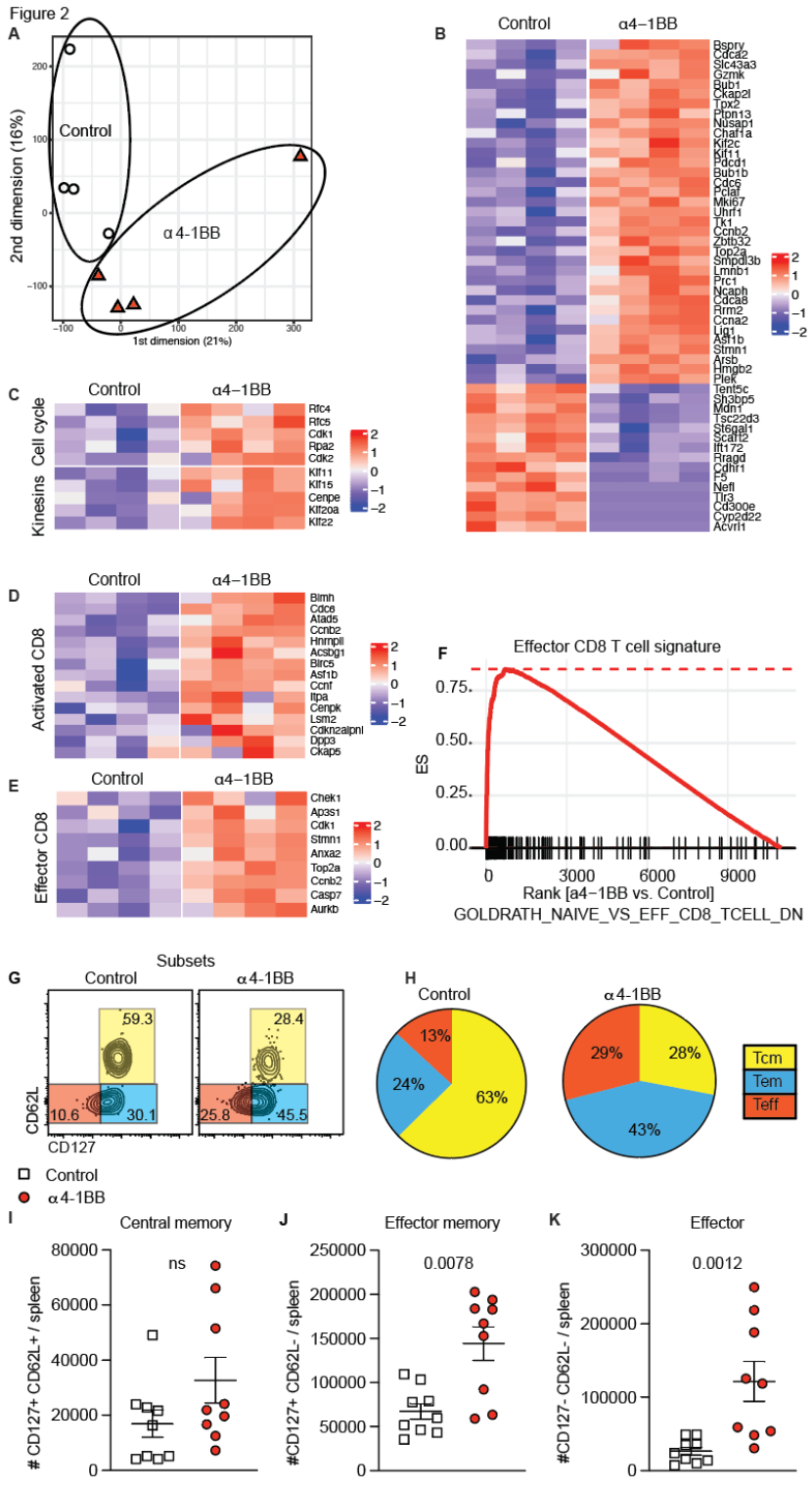

Figure 2. CD8 T cell subset differentiation after reinforcing 4-1BB costimulation. Experimental outline was similar to Figure 1A. At day 7 post-vaccination, splenic CD8 T cells were MACS sorted. Subsequently, live, CD8+, CD44+, K^bVL8 tetramer + cells were FACS-sorted to ~99% purity and used for bulk RNA-seq. (**A**) PCA shows transcriptional clustering. (**B**) Heatmap showing row-standardized expression of selected proliferation and apoptotic genes. (**C**) Heatmap showing row-standardized expression of selected cell cycle (top) and kinesins (bottom) genes. (**D**) Heatmap showing row-standardized expression of selected activation genes. (**E**) Heatmap showing row-standardized expression of selected effector genes.

(**F**) GSEA plots showing enrichment of effector genes. (**G**) Validation of gene expression results at the protein level: Representative FACS plots showing the frequencies of virus-specific CD8 T cells (K^bVL8) that differentiate into effector, effector memory, and central memory T cell subsets. (**H**) Pie diagrams showing CD8 T cell subsets. (**I-K**) Numbers of central memory, effector memory, and effector CD8 T cells. All data are from tetramer+ (K^bVL8+) cells from spleen. RNA-Seq data are from one experiment with n=4 per group. Data from panel H are from one representative experiment with n=4 per group; experiment was performed twice with similar results. All other data are from two experiments with n=4-5 per group/experiment. Indicated P values were calculated by the Mann–Whitney test.

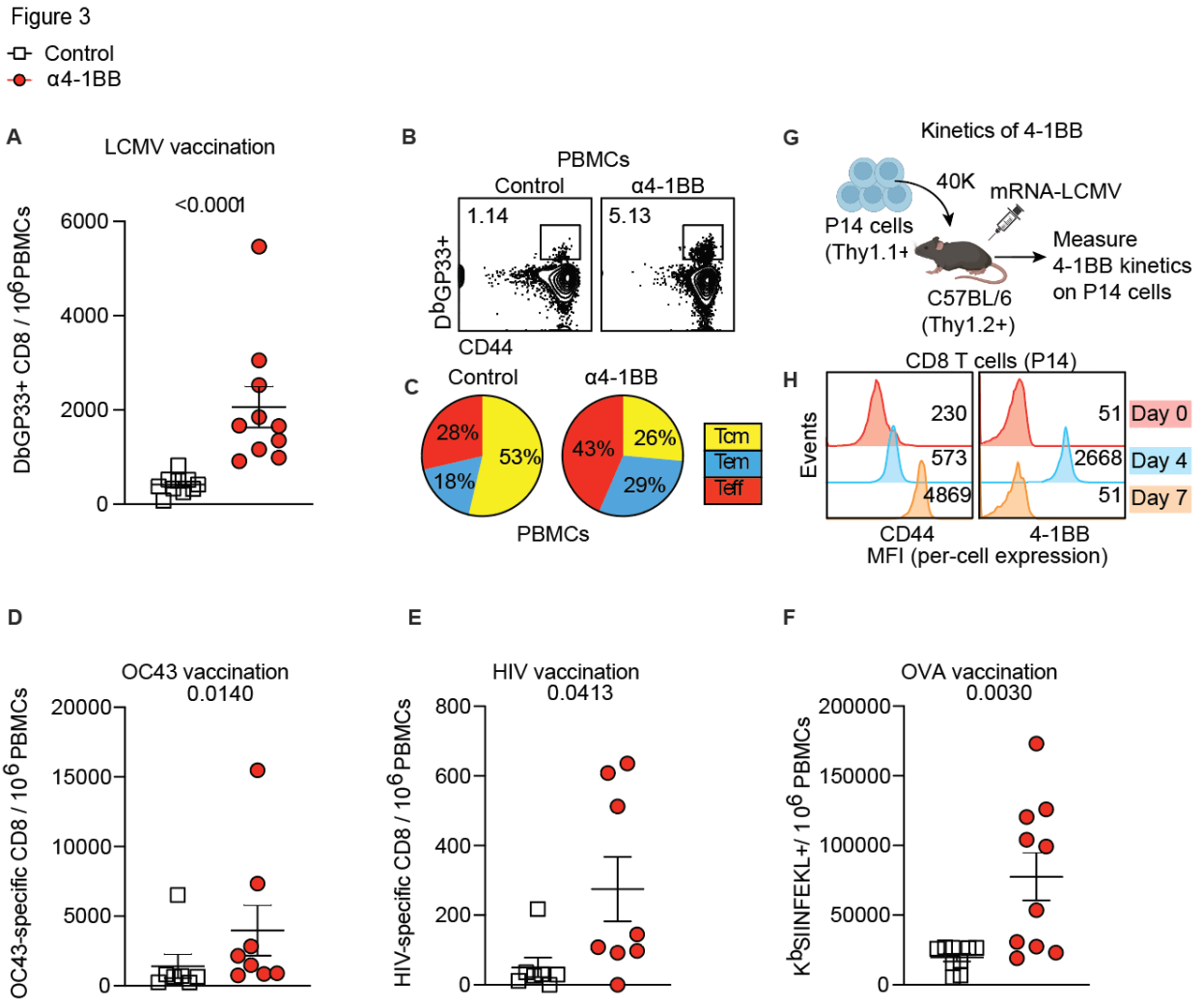

Figure 3. Generalizability to other mRNA vaccines. Mice were immunized with 3 μg of each respective mRNA vaccine followed by treatment with 50 μg of α4-1BB or control antibodies at day 4. (**A**) Summary of LCMV-specific CD8 T cell responses. (**B**) Representative FACS plots of LCMV-specific CD8 T cells. (**C**) Pie diagrams showing CD8 T cell subsets (gated on LCMV-specific CD8 T cells). (**D**) Summary of OC43 spike-specific CD8 T cell responses. (**E**) Summary of HIV env-specific CD8 T cell responses. (**F**) Summary of OVA-specific CD8 T cell responses. Data from panels A-C and F are after tetramer staining; data from panels D-E are after intracellular cytokine stimulation using overlapping peptide pools (IFNγ+). Data from panels A-F are from day 14 post-vaccination, and are from two experiments, one with n=5 per group/experiment and

another one with n=2-5 per group/experiment. (**G**) Experimental outline for measuring 4-1BB following mRNA vaccination. P14 cells were transferred into C57BL/6 mice. One day after transfer, recipient mice were immunized with 3 μg of an mRNA-LCMV GP vaccine, and 4-1BB was measured on P14 cells at various time points. (**H**) 4-1BB on P14 cells after mRNA vaccination**.** Representative histograms showing 4-1BB expression on P14 cells. We utilized this P14 chimera model using a high number of P14 cells to allow us to detect 4-1BB expression on virus-specific CD8 T cells at hyperacute points; endogenous virus-specific CD8 T cells cannot be detected at hyperacute time points due to their low precursor frequency. Mean fluorescence intensity (MFI) is indicated on the x-axis to denote "per-cell expression" of 4-1BB. This adoptive transfer experiment was performed 2 times with n=3 per group, showing similar results (peak of 4-1BB expression at day 4 post-vaccination). All data are shown. Indicated P values were calculated by the Mann–Whitney test.

Figure 4

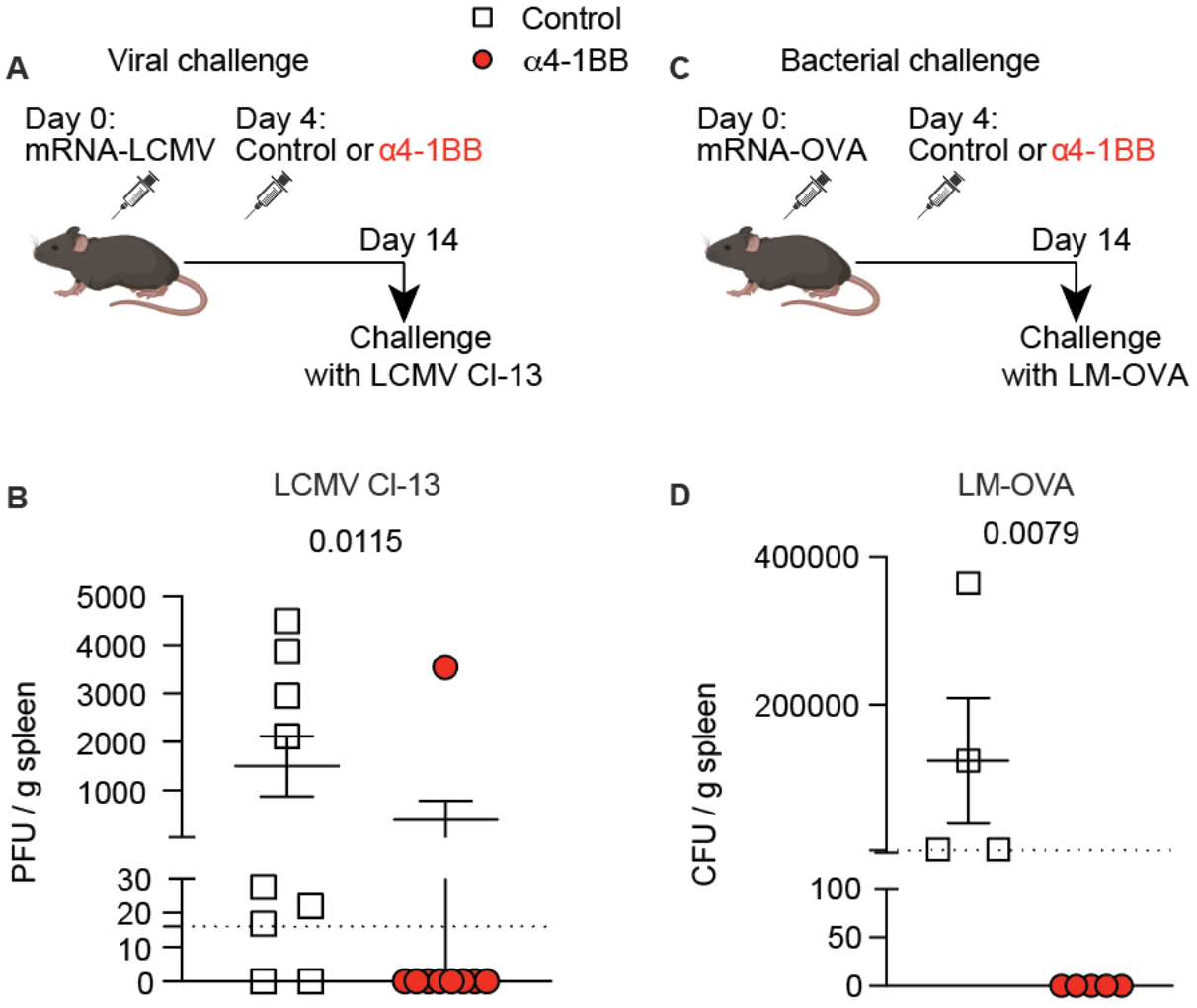

Figure 4. Reinforcing 4-1BB costimulation four days after mRNA vaccination induces sterilizing protection against pathogen challenges. **(A)** Experimental outline to examine if treatment with α4-1BB at day 4 improves immune protection conferred by an mRNA-LCMV vaccine. **(B)** Summary of LCMV Cl-13 loads in the spleen at day 7 post-challenge. At day 14 post-vaccination, mice were challenged i.v. with LCMV Cl-13 ($2x10^6$ PFU) and viral loads were quantified in Vero e6 monolayers. **(C)** Experimental outline to examine if treatment with α4-1BB at day 4 improves immune protection conferred by an mRNA-OVA vaccine. **(D)** Summary of LM-

OVA bacterial loads in the spleen at day 3 post-challenge. At day 14 post-vaccination, mRNA-OVA vaccinated mice were challenged i.v. with a supra-lethal dose of LM-OVA (10^7 CFU) and bacterial loads were quantified in agar plates. In the challenge experiments, mice were immunized with 3 μg of the respective vaccine followed by treatment with 50 μg of α4-1BB or control antibodies at day 4. LCMV Cl-13 challenge data are from two experiments, one with n=5 per group/experiment and another one with n=4 per group/experiment. Data from the LM-OVA challenge experiment are from one experiment, n=4-5 per group. The control vaccines were still able to confer partial protection, relative to no vaccination (mean LCMV Cl-13 viral loads in unvaccinated mice = $1.3x10^7$ PFU/g; mean LM-OVA loads in unvaccinated mice = $1.1x10^6$ CFU/g). Indicated P values were calculated by the Mann–Whitney test.

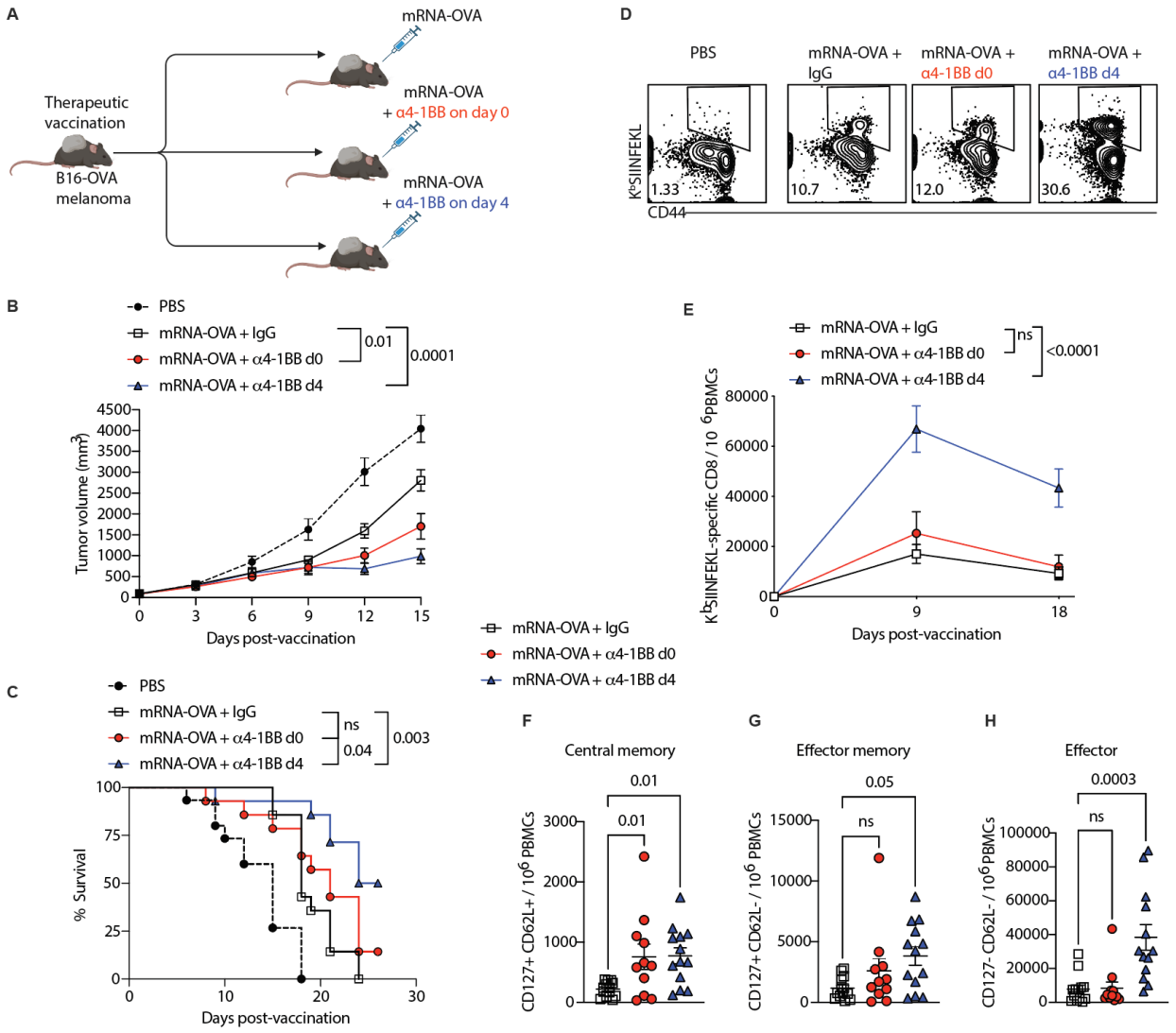

Figure 5. Delayed reinforcement of 4-1BB enhances the efficacy of a therapeutic cancer vaccine. (**A**) Experimental outline to examine if treatment with α4-1BB at day 4 improves immune protection by a therapeutic cancer vaccine. Mice were challenged subcutaneously with $2x10^6$ B16-OVA tumor cells. On day 10 post-tumor challenge, mice were vaccinated intramuscularly with 3 μg of mRNA-OVA. Mice received either control antibodies or α4-1BB (50 μg at day 0 or day 4 after mRNA-OVA vaccination). (**B**) Tumor control. (**C**) Survival. (**D**) Representative FACS plots showing CD8 T cell responses at day 9 post-vaccination. (**E**) Summary of OVA-specific CD8 T cell responses at day 9. (**F-H**) Central memory, effector memory, and effector CD8 T cells

($K^bSIINFEKL$+ PBMCs) at 2 weeks post-vaccination. Data are from two experiments, one with n=6-7 per group and another one with n=8 per group. Indicated P value on panel C was calculated by Log-rank (Mantel-Cox) test, all other p values were calculated by two-way ANOVA (Holm-Šídák's multiple comparisons test).

Figure 6

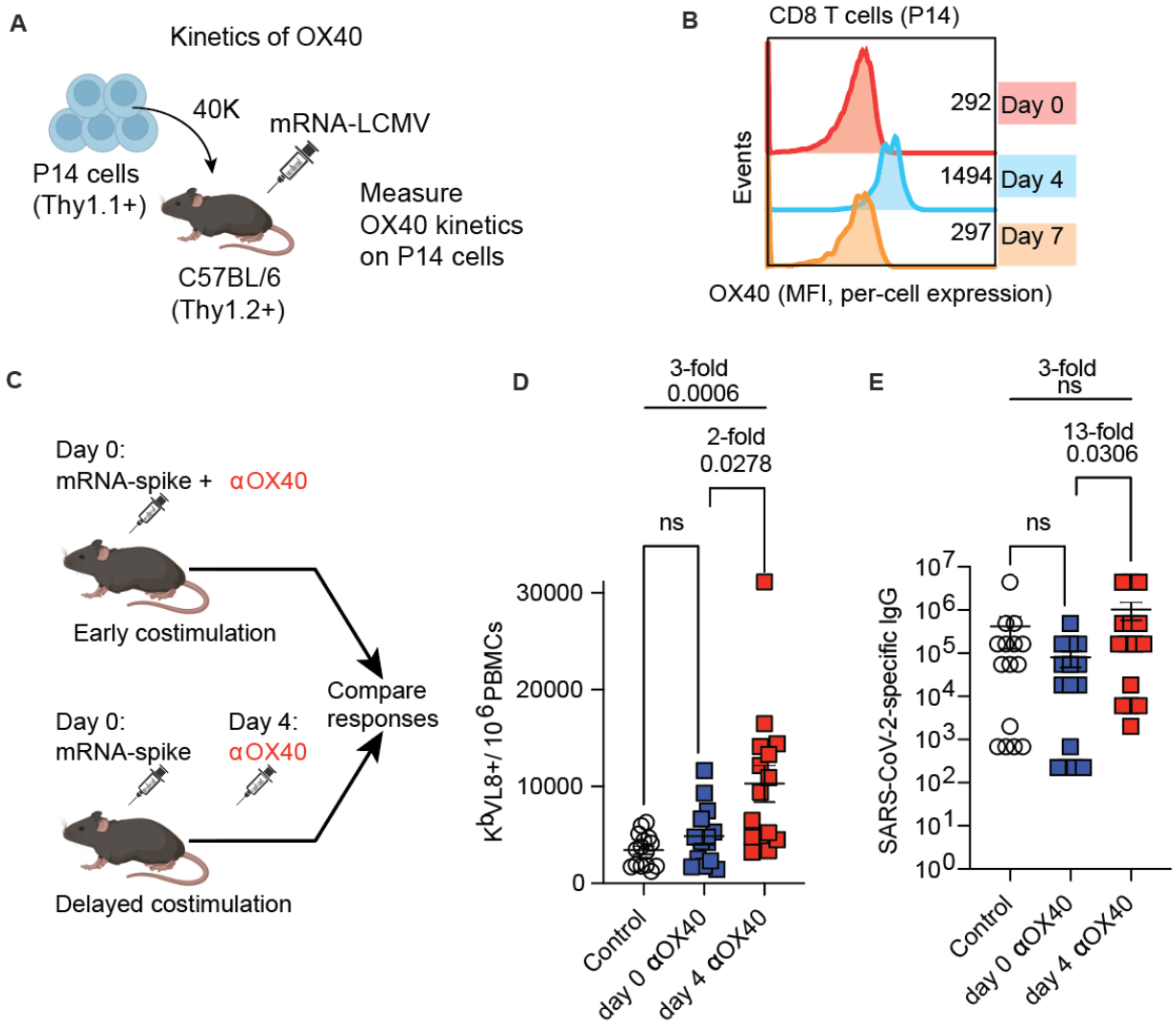

Figure 6. Generalizability to other costimulatory pathways: Reinforcing OX40 costimulation at day 4 results in superior vaccine responses, relative to reinforcing OX40 costimulation at day 0. (A) Experimental outline for evaluating OX40 expression following mRNA vaccination. We utilized the same adoptive transfer model from Figure 3G. **(B)** Kinetics of OX40 on virus-specific CD8 T cells after mRNA vaccination**.** This adoptive transfer experiment was performed 2 times with n=3 per group, showing similar results (peak of OX40 expression at day 4 post-vaccination). **(C)** Time-dependent effects of OX40 costimulation following mRNA vaccination.

Mice were immunized with 3 μg of mRNA-spike vaccine, followed by treatment with OX40 costimulatory antibodies (200 μg of αOX40, clone OX-86) at day 0 or day 4 post-vaccination. CD8 T cell responses (**D**) and antibody responses (**E**) at day 15 post-vaccination are shown. Data in panels D-E are from three experiments, with n=5 per group. Indicated P values were calculated by Kruskal Wallis test (Dunn's multiple comparison).

Supplemental Figures:

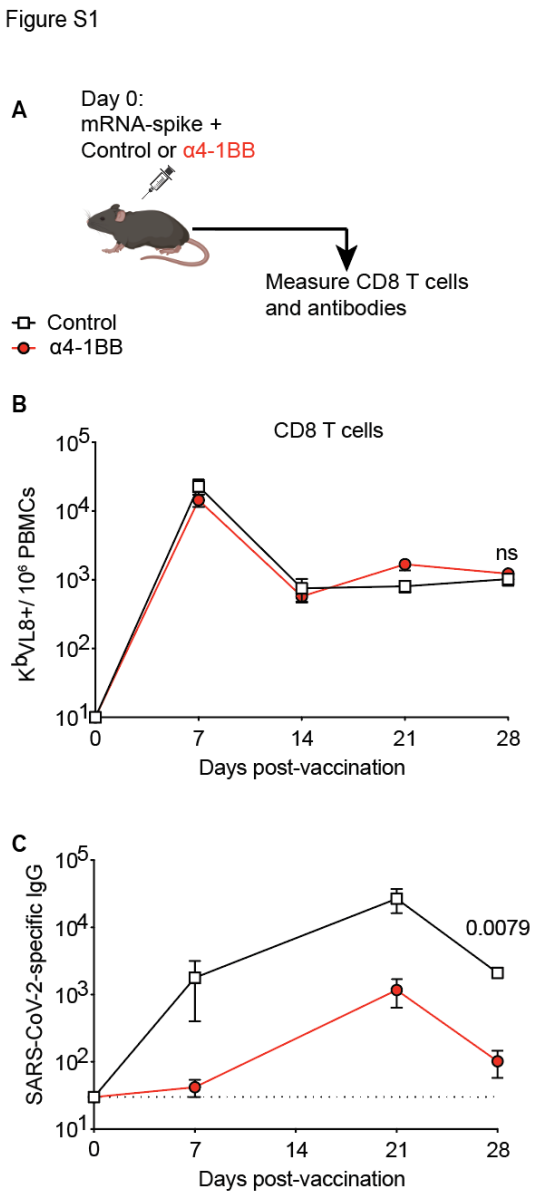

Supplemental Figure 1. Reinforcing 4-1BB costimulation on the same day of vaccination does not improve immune responses. (**A**) Experimental outline for evaluating the effect of α4-1BB at day 0 of vaccination. Mice were immunized with 3 μg of an mRNA-spike vaccine followed by treatment with 50 μg of α4-1BB or control antibodies on the same day. (**B**) Summary of virus-specific CD8 T cells. (**C**) Summary of antibody responses. Data are from one experiment, n=5 per group; experiment was performed twice with similar results. Indicated P values were calculated by the Mann–Whitney test at the last time point.

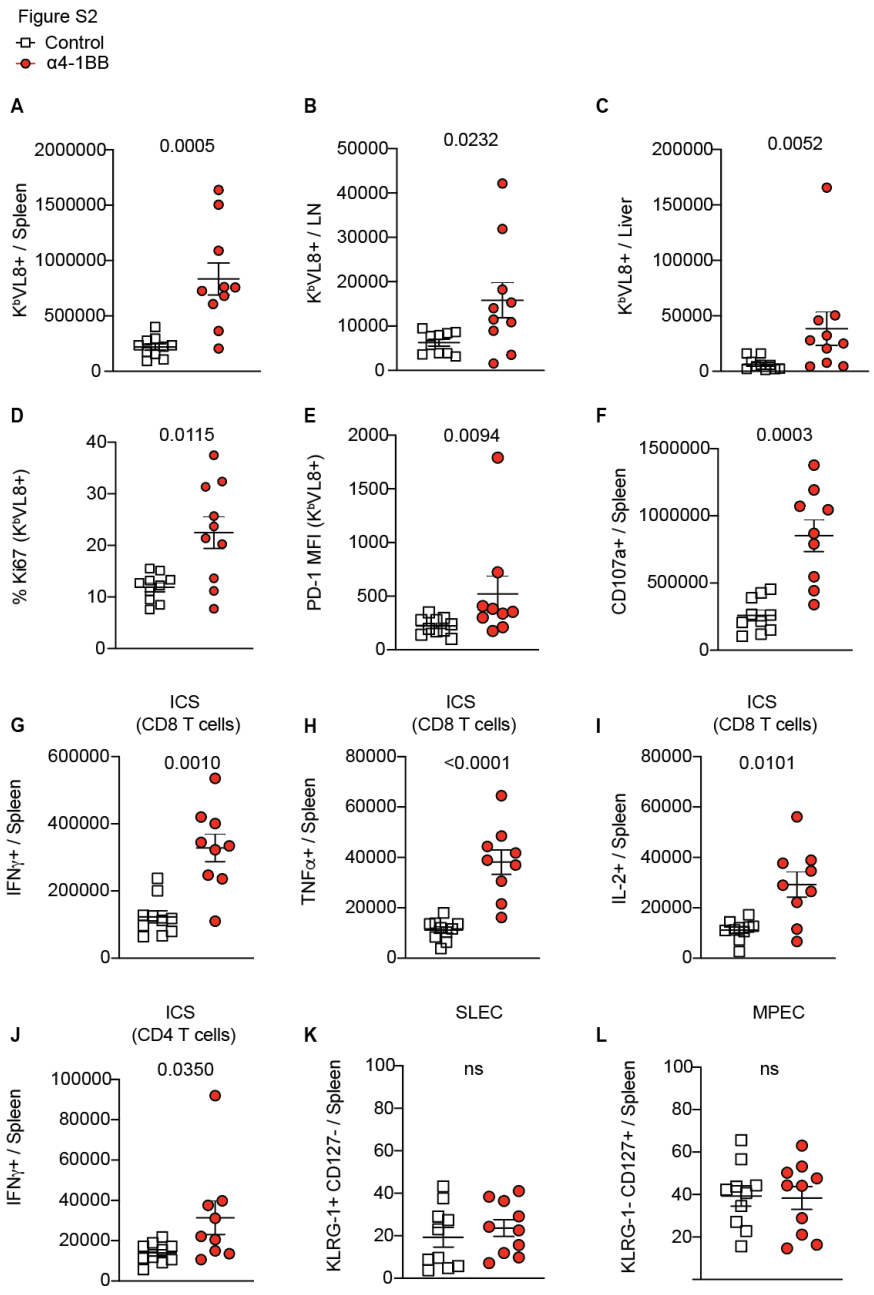

Supplemental Figure 2. Virus-specific CD8 T cells in tissues. Summary of CD8 T cell responses in spleen (**A**), lymph nodes (**B**), and liver (**C**) at day 7 post-vaccination. Summary of Ki67 (**D**) and PD-1 (**E**) expression on splenic CD8 T cells. Summary of CD107a (**F**), IFNγ (**G**), TNFα (**H**), IL-2 (**I**) on virus-specific CD8 T cells. Summary of IFNγ (**J**) on virus-specific CD4 T cells. Data from panels F-J are from intracellular cytokine staining (ICS) at day 15 post-vaccination, using spike overlapping peptide pools in the presence of GolgiPlug and GolgiStop. Summary of SLEC and MPEC subsets on splenic CD8 T cells (K^bVL8+) at day 30 post-vaccination. Mice were immunized with 3 μg of an mRNA-spike vaccine followed by treatment with 50 μg of α4-1BB or control antibodies. Data are from two experiments, n=5 per group/experiment. Indicated P values were calculated by the Mann–Whitney test.

Figure S3

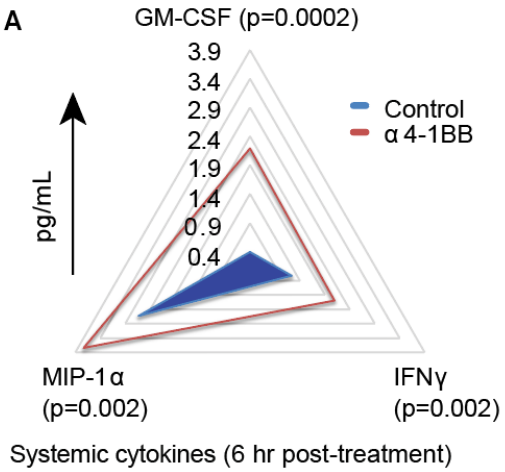

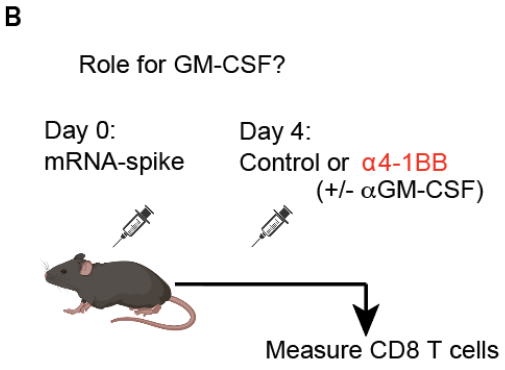

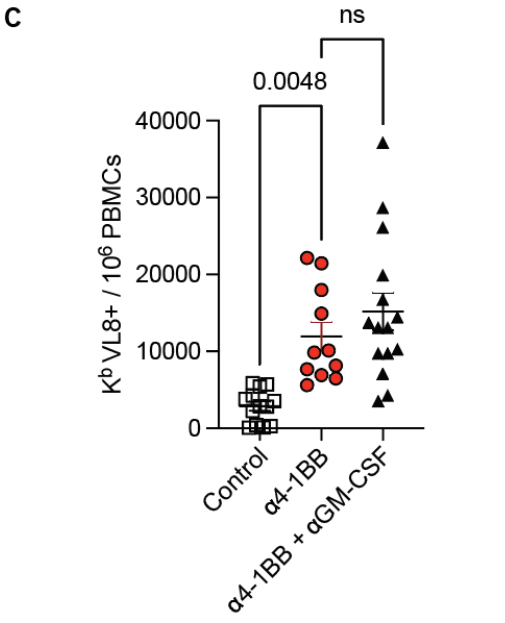

Supplemental Figure 3. Systemic cytokines after treatment with 4-1BB costimulatory antibodies. (A) Radar plots showing cytokines in serum 6 hr after treatment with 4-1BB costimulatory antibodies. 4-1BB costimulatory antibodies were administered at day 4 post-vaccination, same as in Figure 1C, and cytokines were quantified 6 hr after treatment. Data are from two experiments, n=5 per group/experiment. All data are shown. Indicated P values were calculated by the Mann–Whitney test. (**B**) Experimental outline for evaluating the mechanistic role of GM-CSF in the improvement of CD8 T cells following treatment with α4-1BB. (**C**) Summary of CD8 T cell responses in blood at day 14 post-vaccination. Data are from two experiments, n=3-5 per group/experiment. All data are shown. Indicated P values in panel C were calculated by one-way ANOVA (multiple comparisons).

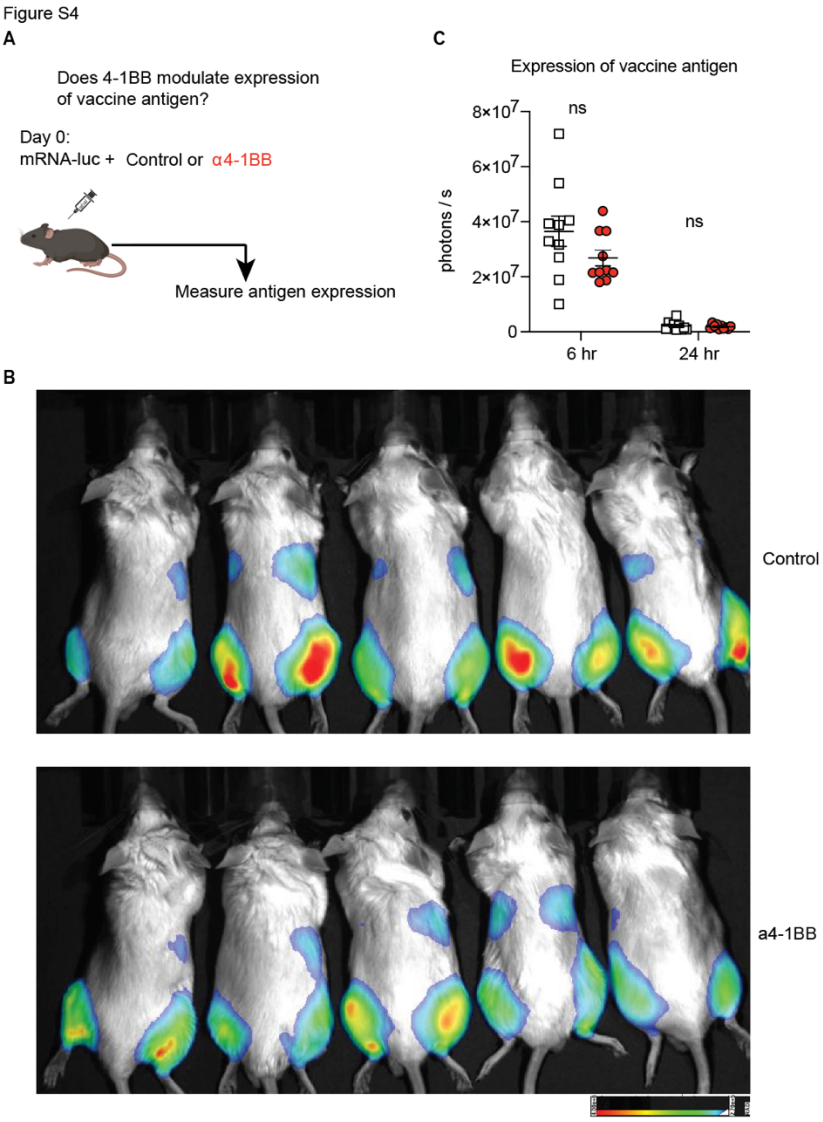

Supplemental Figure 4. 4-1BB costimulation does not significantly affect antigen expression following mRNA vaccination. **(A)** Experimental outline for quantifying antigen expression following reinforcement of 4-1BB costimulation. We utilized BALB/c mice, since their white coat facilitates visualization by bioluminescence. BALB/c mice were immunized intramuscularly with 3 μg of an mRNA-luciferase, and after 30 min, they were treated intraperitoneally with 50 μg of α4-1BB or control antibodies. After 6 hr post-immunization, mice were injected intraperitoneally with luciferin and luciferase expression was quantified by in vivo bioluminescence. (**B**) Bioluminescence images at 6 hr post-immunization. (**C**) Summary of antigen expression by bioluminescence. Data are from one experiment, n=5 per group/experiment (each quadriceps represents a separate immunization site, equating 10 quadriceps per group). All data are shown. Indicated P values were calculated by the Mann–Whitney test.

Figure S5

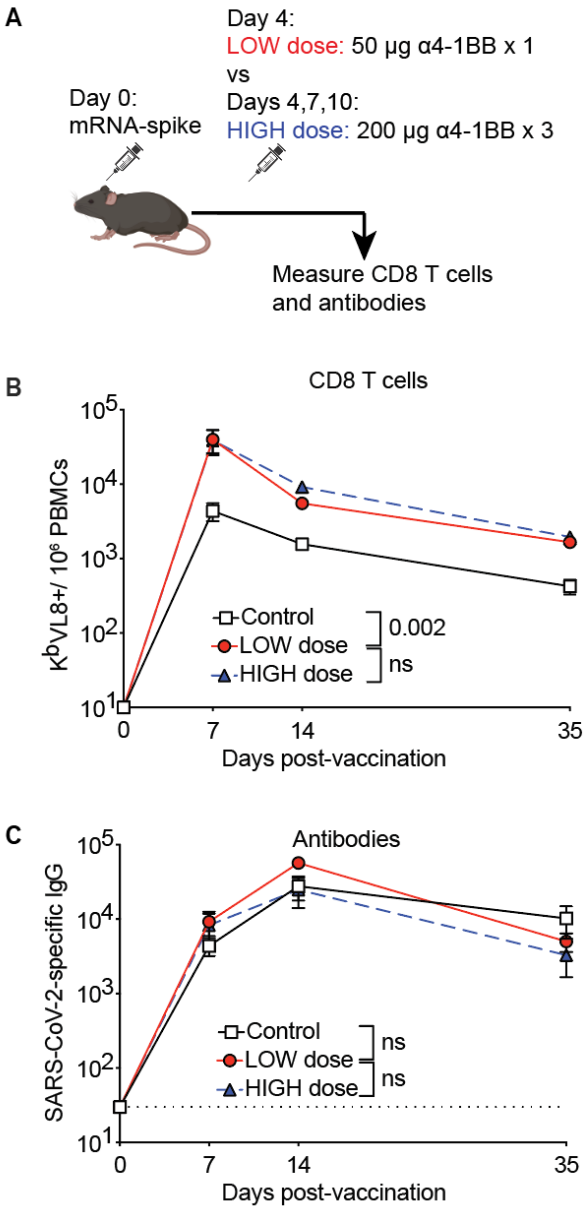

Supplemental Figure 5. Continuously treating with α4-1BB after day 4 does not result in superior responses relative to treating just once at day 4. (**A**) Experimental outline for comparing the effects of α4-1BB dose. Mice were vaccinated with 3 µg of an mRNA-spike vaccine. One group of mice received a single dose of 50 µg of α4-1BB on day 4 (**LOW dose**); another group of mice received 200 µg of α4-1BB on days 4, 7, and 10 (**HIGH dose**). (**B**) Summary of virus-specific CD8 T cell responses in PBMCs. (**C**) Summary of antibody responses in sera. Data are from one experiment with n=5 per group. Indicated P values were determined by 2-way ANOVA (Dunnett's multiple comparisons tests) at the last time point.

Figure S6

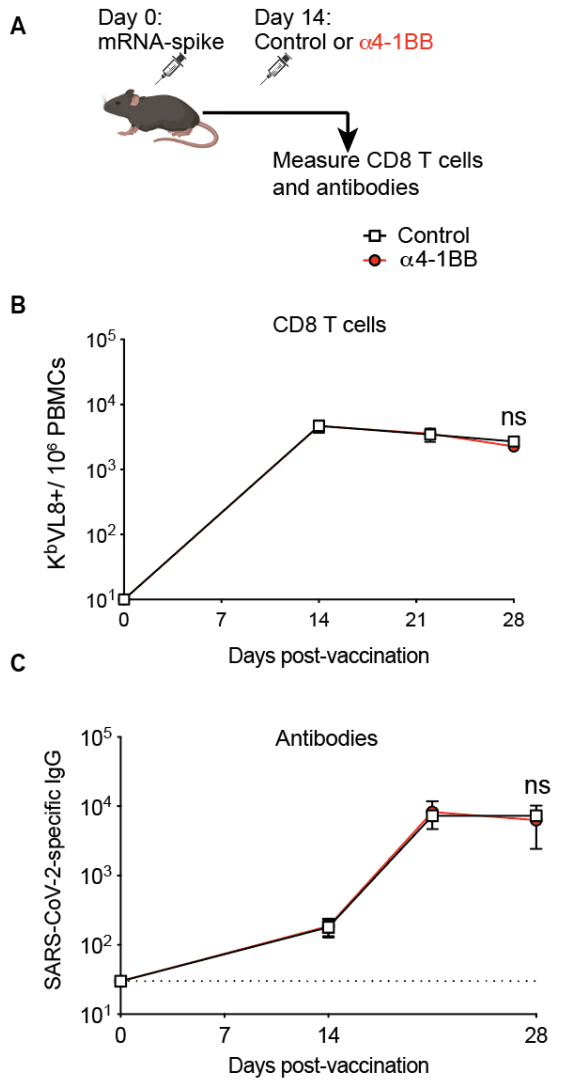

Supplemental Figure 6. 4-1BB costimulation after day 14 does not result in improvement of immune responses following mRNA-SARS-CoV-2 vaccination. (A) Experimental outline for evaluating whether treatment with α4-1BB after 2 weeks improves immune responses elicited by an mRNA-spike vaccine. C57BL/6 mice were immunized with 3 µg of an mRNA-spike vaccine followed by treatment with 50 µg of α4-1BB or control antibodies at day 14. **(B)** Summary of virus-specific CD8 T cell responses in PBMCs. (**C**) Summary of antibody responses in sera. Data are from one experiment with n=5 per group. Indicated P values were calculated by the Mann–Whitney test at the last time point.

Figure S7

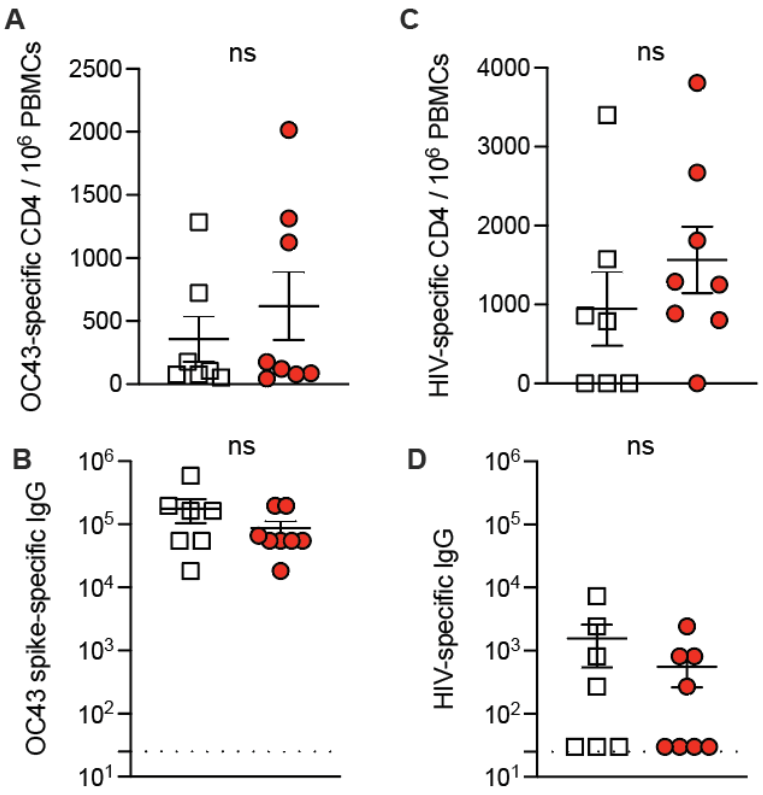

Supplemental Figure 7. CD4 T cell and antibody responses are not significantly different following treatment with 4-1BB costimulatory antibodies at day 4. (A) Summary of OC43 spike-specific CD4 T cell responses in PBMCs. **(B)** Summary of OC43 spike-specific antibody responses in sera. **(C)** Summary of HIV env-specific CD4 T cell responses in PBMCs. **(D)** Summary of HIV env-specific antibody responses in sera. Mice were immunized with 3 μg of each respective mRNA vaccine followed by treatment with 50 μg α4-1BB or control antibodies at day 4. Data from panels A and C are after intracellular cytokine stimulation using overlapping peptide pools (IFNγ+). Data are from day 14 post-vaccination. Data are from two experiments, one with n=5 per group/experiment and another one with n=2-3 per group/experiment. All data are shown. Indicated P values were calculated by the Mann–Whitney test.

Figure S8

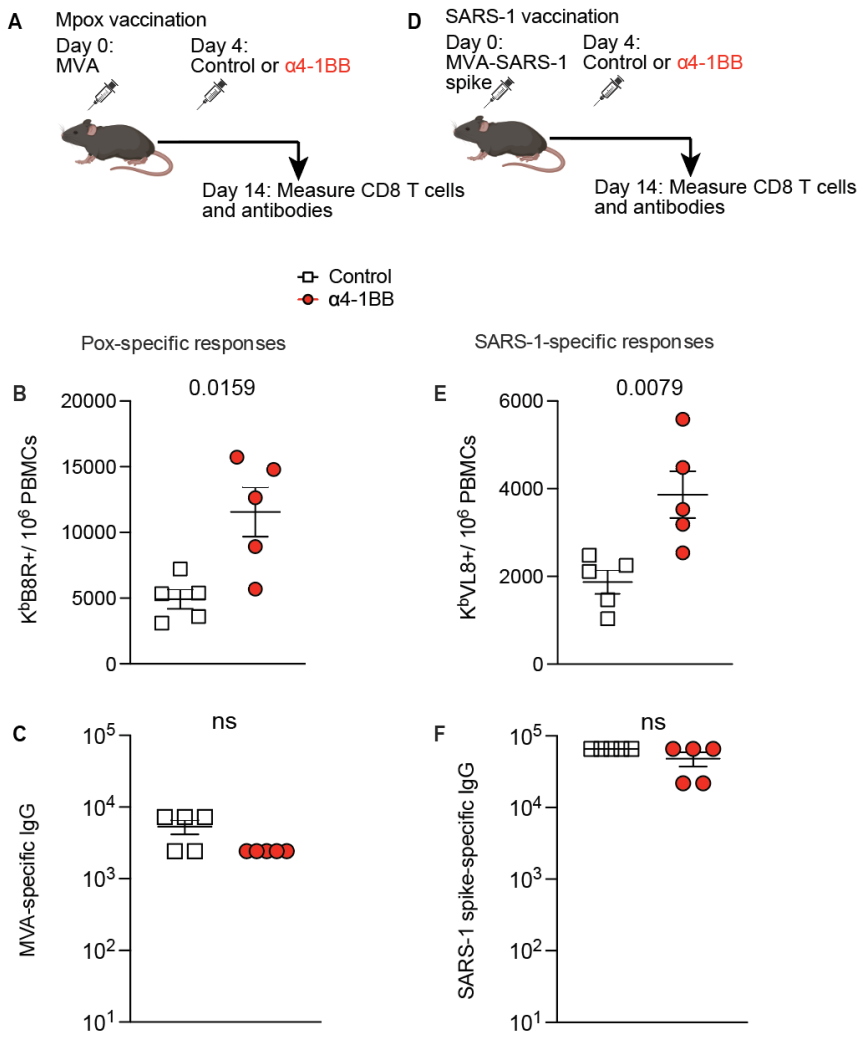

Supplemental Figure 8. Generalizability to another vaccine platform: a poxvirus vector. (A) Experimental outline for evaluating whether treatment with α4-1BB improves immune responses elicited by an MVA vaccine. **(B)** Summary of MVA-specific CD8 T cell responses in PBMCs. **(C)** Summary of MVA-specific antibody responses in sera. **(D)** Experimental outline for evaluating whether treatment with α4-1BB improves immune responses elicited by an MVA-SARS-CoV-1 vaccine. **(E)** Summary of SARS-CoV-1 specific CD8 T cell responses in PBMCs. **(F)** Summary of SARS-CoV-1-specific antibody responses in sera. Mice were vaccinated with 10^7 PFU of the respective MVA vector followed by treatment with 50 µg of α4-1BB or control antibodies at day 4. Data are from day 14 post-vaccination. Data are from one experiment, n=5 per group. Indicated P values were calculated by the Mann–Whitney test.

Figure S9

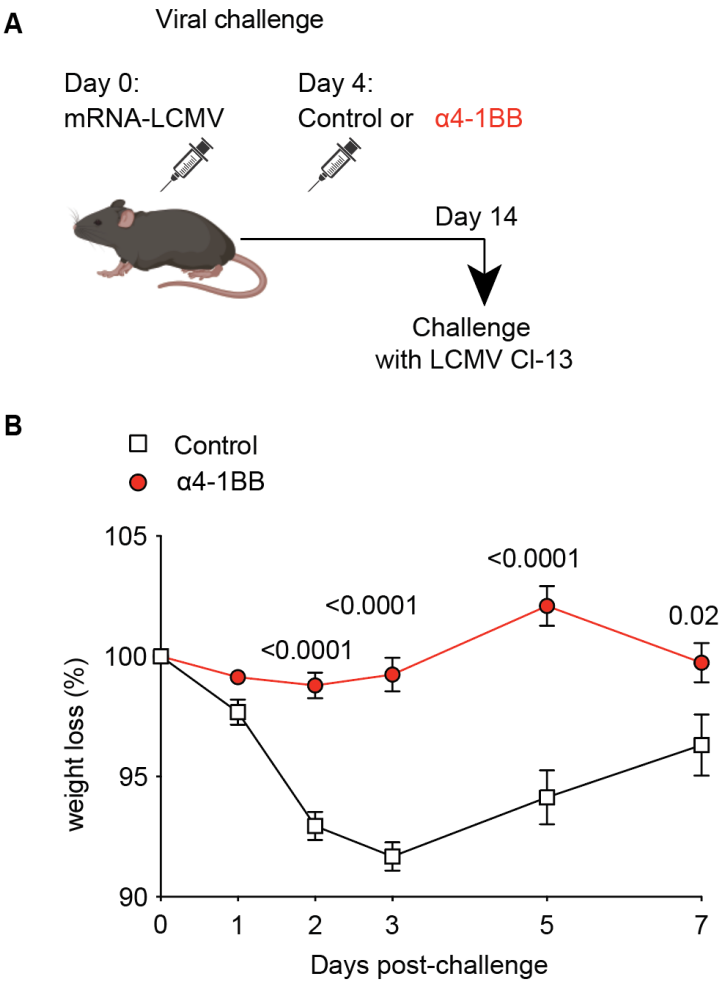

Supplemental Figure 9. Reinforcing 4-1BB costimulation 4 days after mRNA-LCMV vaccination prevents weight loss after chronic LCMV Cl-13 challenge. (A) Experimental outline to examine if treatment with α4-1BB at day 4 improves immune protection conferred by an mRNA-LCMV vaccine (same mice from Figure 4A-4B). **(B)** Summary of weight loss after LCMV Cl-13 challenge. Data are from two experiments, each with n=5 per group/experiment. Indicated P values were calculated by the Mann–Whitney test.

Figure S10

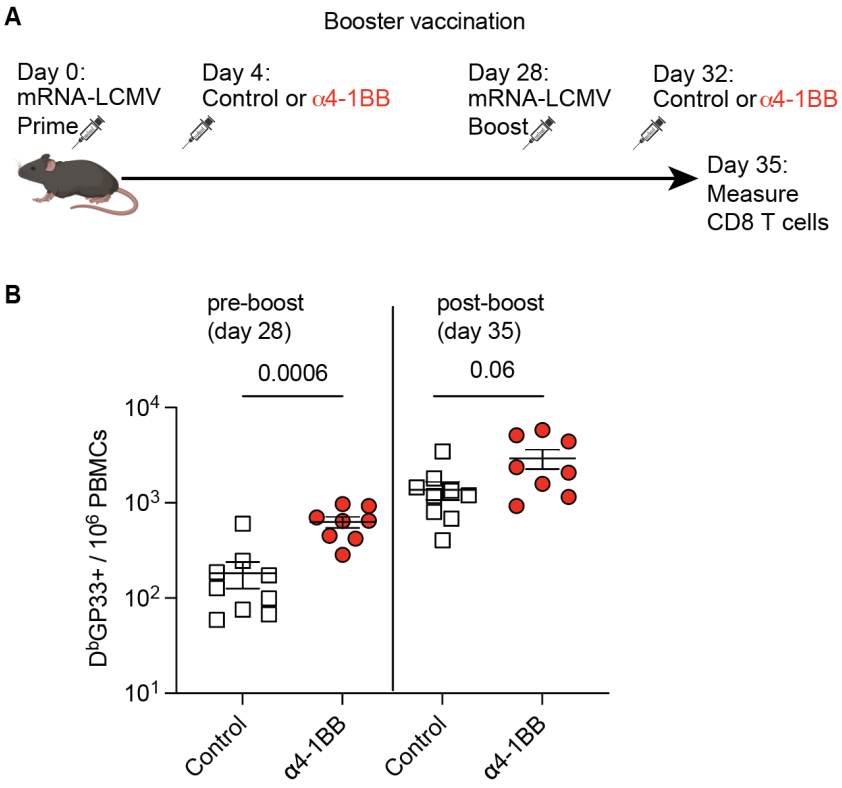

Supplemental Figure 10. Effect of reinforcing 4-1BB costimulation in a prime-boost vaccine regimen. (A) Experimental outline to examine the effects of α4-1BB during a recall response. Mice were primed with 3 μg of an mRNA-LCMV vaccine followed by treatment with 50 μg of α4-1BB or control antibodies at day 4 post-prime. At day 28 post-prime, mice were boosted homologously and treated with 50 μg of α4-1BB or control antibodies at day 4 post-boost. (**B**) Summary of LCMV-specific CD8 T cell responses in PBMCs. Data are from two experiments, with n=4-5 per group/experiment. All data are shown. Indicated P values were calculated by the Mann–Whitney test.

Figure S11

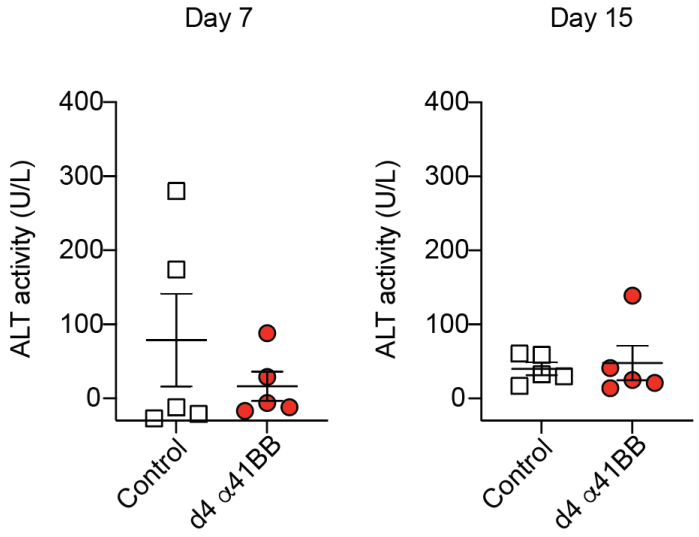

Supplemental Figure 11. Treatment with α4-1BB antibody at day 4 post-vaccination does not increase alanine aminotransferase (ALT) activity in sera relative to control vaccinated mice. Mice were immunized with 3 μg of mRNA-spike vaccine followed by treatment with a single dose of α4-1BB (50 μg) or control antibodies at day 4. ALT activity was quantified in sera after vaccination. Data are from one experiment, with n=5 per group. Indicated P values were calculated using the Mann–Whitney test.

Figure S12

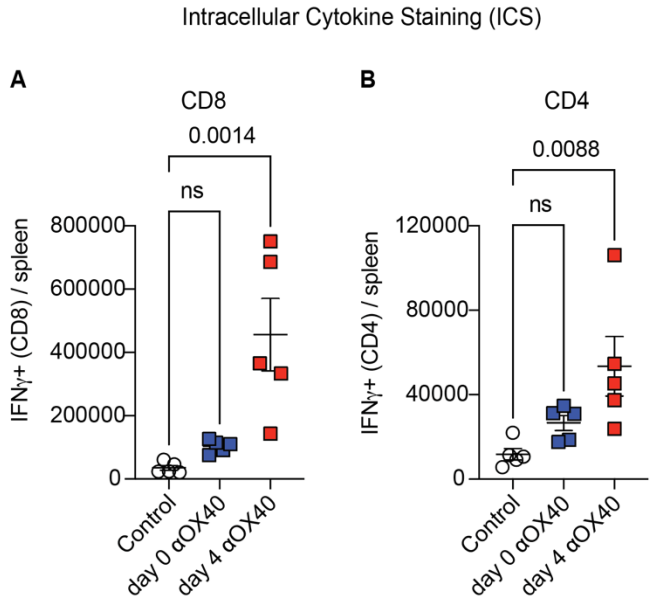

Supplemental Figure 12. Cytokine expression on virus-specific CD8 and CD4 T cells after reinforcing OX40 costimulation. The experimental outline was identical to that of Figure 6C. Splenic CD8 T cells (**A**) and CD4 T cells (**B**) responses at day 30 post-vaccination are shown. Data are after intracellular cytokine stimulation using overlapping peptide pools (IFNγ+). Data are from one experiment, with n=5 per group. Indicated P values were calculated by the Mann–Whitney test.

Figure S13

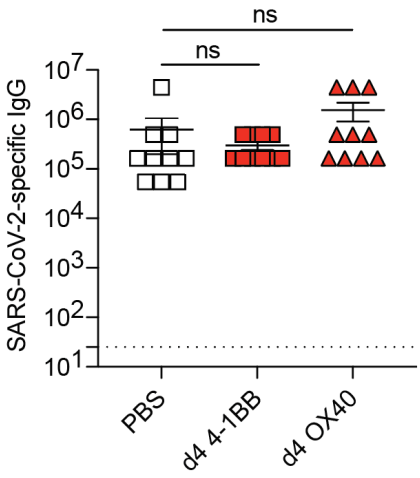

Supplemental Figure 13. Comparative analyses of antibody responses following α4-1BB or αOX40 treatment. The experimental outline was identical to that of Figs. 1A and 6C. Antibody responses in sera at day 15 post-vaccination are shown. Data are from two experiments, with n=5 per group. Indicated P values were calculated by the Kruskal Wallis test (Dunn's multiple comparisons).